Marine and Petroleum Geology 122 (2020) 104599

Contents lists available at ScienceDirect

Marine and Petroleum Geology

journal homepage: www.elsevier.com/locate/marpetgeo

Research paper

A three-dimensional (3D) structural model for an oil-producing basin of the Brazilian equatorial margin

Narelle Maia de Almeida [a,*], Tiago M. Alves [b], F. Nepomuceno Filho [c], George Satander Sá Freire [a,d], Ana Clara B. Souza [d], Karen M. Leopoldino Oliveira [d], Márcio Nunes Normando [d], Thiago Henrique S. Barbosa [e]

[a] Departamento de Geologia, Universidade Federal do Ceará (UFC), Campus do Pici, Bloco 912, Fortaleza, Ceará, CEP 60440-554, Brazil
[b] Cardiff University. 3D Seismic Lab, School of Earth and Ocean Sciences, Cardiff University, Cardiff, United Kingdom
[c] Departamento de Física, Universidade Federal do Ceará (UFC), Campus do Pici, Bloco 922, Fortaleza, Ceará, CEP 60440-554, Brazil
[d] Programa de Pós-Graduação em Geologia, Universidade Federal do Ceará (UFC), Campus do Pici, Bloco 912, Fortaleza, Ceará, CEP 60440-554, Brazil
[e] Departamento de Engenharia do Petróleo, Universidade Federal do Ceará (UFC), Campus do Pici, Bloco 709, Fortaleza, Ceará, CEP 60440-554, Brazil

ARTICLE INFO

Keywords:
Atlantic ocean
Equatorial Brazil
Ceará basin
3D seismic
Oil fields
3D modelling

ABSTRACT

Hydrocarbon discoveries in Equatorial Brazil, Equatorial Africa and French Guiana-Suriname-Guyana have recently confirmed their importance as new exploration frontiers. The Mundaú sub-basin, located on the Brazilian Equatorial Margin, comprises four producing fields in shallow waters: Xaréu, Atum, Espada e Curimã. In order to understand the structural and seismic-stratigraphic frameworks of an oil-producing region in Equatorial Brazil, this work addresses the 3D geometry and spatial distribution of main faults in the Curimã and Espada fields. The occurrence of hydrocarbons in the Mundaú sub-basin is compared with fields in other parts of the Brazilian Equatorial Margin and Equatorial Africa. Data from 12 wells and a 3D post-stack time-migrated multichannel seismic volume are used to define nine (9) seismic-stratigraphic units: the syn-rift Mundaú Formation (Units 1, 2, 3 and 4); the transitional Paracuru Formation (Unit 5); and the drift Ubarana (Uruburetama and Itapagé Members, Units 6 and 7), Tibau and Guamaré Formations (Units 8 and 9). The study area is dominated by NW-SE planar normal faults, basinward-dipping, that form multiple half-grabens, and tilted blocks with small anticlines and synclines genetically related to a transtensional system. Three types of plays are recognised in the Mundaú sub-basins: structural, combined (structural-stratigraphic) and stratigraphic (turbiditic). In the eastern part of the study area, where the basement is shallow, no oil was found. Conversely, oil was discovered in an anticlinal trap formed over a hanging-wall block analogous to fields on the Côte D'Ivoire-Ghana transform margin. This work shows that combined traps on footwall blocks are successful plays near the shelf break of the Mundaú sub-basin, in similarity with the Espoir and Baobab fields in Ivory Coast. Furthermore, turbiditic reservoirs in drift units are analogous to the Stabroek block in Guyana and prospects in the Gulf of Guinea. The structural and petroleum-play analyses in this work are therefore crucial to understand the multiple geological processes leading to the trapping of hydrocarbons in the larger Equatorial Atlantic Ocean.

1. Introduction

The Ceará Basin is located on the Brazilian Equatorial Margin (BEM) between the Potiguar Basin to the southeast and the Barreirinhas Basin to the northwest (Fig. 1). The BEM developed as a typical continental margin of the transform type (Matos, 2000). The bulk of its development was dominated either by oblique extension (transtension) or by pure and simple shear movements, all responding to a dominant dextral sense of movement in transfer (syn-rift) and transform (post-rift) faults. In this portion of the late Gondwana supercontinent, continental rupture and breakup took place in an East-West direction, creating shorelines with two predominant directions: NW-SE in transtensional portions, and E-W

* Corresponding author.
E-mail addresses: narelle@ufc.br (N. Maia de Almeida), alvest@cardiff.ac.uk (T.M. Alves), nepomuceno@fisica.ufc.br (F. Nepomuceno Filho), freire@ufc.br (G.S.S. Freire), anaclarageologia@alu.ufc.br (A.C.B. Souza), karenleopoldino@gmail.com (K.M. Leopoldino Oliveira), mnormando@gmail.com (M.N. Normando), thiagohenrique@alu.ufc.br (T.H.S. Barbosa).

https://doi.org/10.1016/j.marpetgeo.2020.104599
Received 3 January 2020; Received in revised form 31 May 2020; Accepted 15 July 2020
Available online 22 July 2020

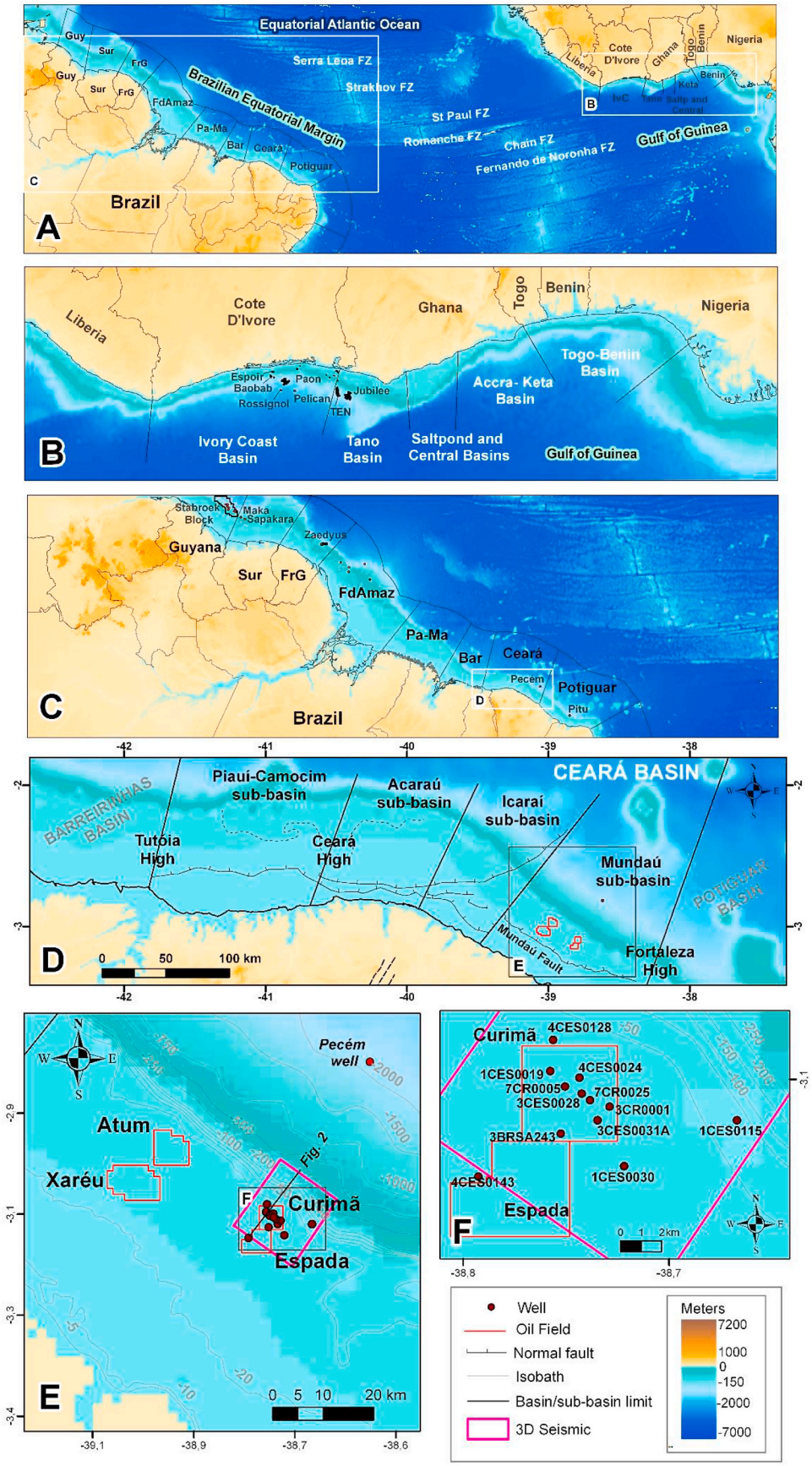

Fig. 1. A) Map of the Equatorial Atlantic Ocean highlighting location of fracture zones and marginal basins (Guy: Guyana, Sur: Suriname, FrG: French Guiana, FdAmaz: Foz do Amazonas, Pa-Ma: Pará-Maranhão, Bar: Barreirinhas, IvC: Ivory Coast, Saltp: Saltpond). B) Gulf of Guinea basins, their oil fields, and hydrocarbon discoveries mentioned in this work. C) Fields and discoveries of the Brazilian Equatorial Margin, French Guiana, Suriname and Guyana. D) Ceará Basin sub-divided into four sub-basins: Piauí-Camocim, Acaraú, Icaraí and Mundaú. The study area is located in the Mundaú sub-basin. Structural data was compiled from Zalán and Warme (1985) and Morais Neto et al. (2003). Basin boundaries were provided by the Brazilian National Agency of oil, gas and biofuels (ANP), while the boundaries of sub-basins were based on Morais Neto et al. (2003). E) Relative location of the four producer fields (Xaréu, Atum, Curimã and Espada) of the Mundaú sub-basin. The location of the wells and 3D seismic data are shown. F) Details of the well data used in this study, as provided by the ANP. The topographic model in the figure was provided by NOAA (ETOPO1).

in purely transcurrent portions (Zalán, 2015).

The Ceará Basin has been considered, since the 1970's, to be a modest oil and gas producer in shallow waters, where production rates have reached only a few thousands of boe/d. In contrast, the neighbouring Potiguar Basin recorded significant yields during the 1990s, with its onshore fields reaching a production rate of ~100,000 boe/d. The onshore portion of the Barreirinhas Basin also reached production rates of a few tens of thousands of boe/d into the 1980s; however, there is no significant production in this basin at present, as well as in other basins of the BEM such as Pará-Maranhão and Foz do Amazonas (ANP, 2020) (Fig. 1). More recently, in 2012, Petrobras (Petróleo Brasileiro SA) drilled the Pecém well to announce the first ever deep-water oil discovery in the Ceará Basin. Subsequently, Maia de Almeida et al. (2020) proved that reservoirs in the Pecém well comprise Cretaceous sandstones in a combined trap related to both an erosional unconformity and a normal fault. Leopoldino Oliveira et al. (2020) later identified a series of potential stratigraphic and structural traps, in rift and drift sequences of the Ceará Basin. The first deep-water discovery in Potiguar Basin occurred in 2013 with the drilling of the Pitu well. Soon after, the Brazilian Agency of Petroleum (ANP) opened new exploratory opportunities in structured sandstones of Aptian age, and in Upper Cretaceous, Paleogene and Neogene turbidite sequences in the Potiguar Basin (ANP, 2018).

On the African conjugate margin of the BEM, the Gulf of Guinea Province (Côte d'Ivoire, Ghana, Togo, and Benin) towards the western part of the coast of Nigeria, relatively little hydrocarbon exploration occurred before the 1990s. Until 1995, most discoveries were located in water depths of less than 500 m (Brownfield and Charpentier, 2006). In the 2000s, new discoveries in deep-water areas of Equatorial Africa were made public. The first deep-water discovery in Equatorial Africa was the Baobab field off the Ivory Coast (2005). Two years later the discovery of the giant Jubilee field, offshore Ghana, drew attention to the whole of the Equatorial Atlantic as a major hydrocarbon province. The Jubilee field is now producing more than 100,000 boe/d and has a planned peak production of 120,000 boe/d (Dailly et al., 2017). Further increasing the importance of the Equatorial Atlantic as a petroleum province, the Tweneboa-Enyenra-Ntomme (TEN) fields in Ghana's deep-water margin were discovered between 2009 and 2012, and began producing oil in 2016 at relatively large rates of 80,000 boe/d.

Offshore French Guyana, significant discoveries have included the Zaedyus Field (2011) with recoverable reserves of 130×10^6 toe (Huaicun, 2014), and the Lisa field of the Stabroek Block, drilled in 2015, this latter comprising potential recoverable reserves of $109–191 \times 10^6$ toe (OGJ, 2020). Other successful discoveries in the Stabroek Block included the Payara, Liza deep, Snoek and Turbot fields (2017), the Ranger, Pacora, Longtail, Hammerhead and Pluma fields (2018), the Tilapia, Haimara, Yellowtail and Tripletail fields (2019); and the Mako field of 2020 (Exxon Mobil, 2020). More recently, the Maka and Sapakara discoveries offshore Suriname led to the identification of, at least, seven distinct play types (Offshore, 2020).

Most oil and gas discoveries on Equatorial margins of the Central Atlantic are associated with the presence of stratigraphic traps in turbidites. Structural and combined traps are also present (Dailly et al., 2017; Jianping et al., 2010; Kelly and Doust, 2016; Maia de Almeida et al., 2020; Tetteh, 2016; Yang and Escalona, 2011). In such a setting, faults have an important role with regards to controlling oil migration from source intervals to main reservoirs. Faults can act as either conduits or barriers for hydrocarbon migration because they have anisotropic flow properties owing to their complicated three-dimensional structure (Jiang et al., 2015). Thus, a predictive knowledge of fault zone structure and transmissibility can have an enormous impact on the economic viability of new exploration targets, resulting in significant benefits during reservoir management. Understanding the effects of faults and fractures on fluid flow behaviour and distribution within hydrocarbon provinces has, therefore, become a priority in many an offshore prospect (Knipe et al., 1998).

Costa et al. (1990) have shown that hydrocarbon plays in shallow waters of the Ceará Basin are of the stratigraphic (turbiditic), combined (structural-stratigraphic) and structural types. Structural plays may be classified as rotational, transpressional, transtensional or footwall-related. In addition, Pessoa Neto (2004) showed that the Atum and Curimã oil fields in the Mundaú sub-basin comprise classical examples of combined traps generated by the erosional truncation of tilt blocks limited by normal faults. Though Pessoa Neto (2004) was able to demonstrate that hydrocarbon traps are usually of the mixed type (structural-stratigraphic), and others several structural interpretations have been proposed for the area based on 2D seismic data (Costa et al., 1990; Matos et al., 1996; Morais Neto et al., 2003; Antunes, 2004; Pessoa Neto, 2004; Medeiros et al., 2007; Antunes et al., 2008; Maia de Almeida et al., 2020; Leopoldino Oliveira et al., 2020), the geometry and distribution of subsurface faults is still poorly known in the larger Ceará Basin. Against such a backdrop, this work aims at recognising the 3D geometry and spatial distribution of faults in the Mundaú sub-basin, Ceará Basin, and explain their control on the occurrence of hydrocarbons in the area encompassing the Curimã and Espada fields (Fig. 1). The results will be compared to other basins of the BEM and Equatorial Africa. Three-dimensional (3D) seismic data and a suite of exploration wells are therefore used to address fundamental research questions:

a) What are the typical fault geometries in the Curimã and Espada fields? How are they distributed in these two subsurface prospects?
b) How structural elements in the Mundaú sub-basin fit within the regional context of continental rifting of the Equatorial Atlantic Ocean?
c) In what way(s) these structures influence local petroleum plays and subsequent hydrocarbon accumulations in an economically significant region of Equatorial Brazil?
d) How the present findings compare with similar petroleum basins elsewhere in Equatorial areas of the Central Atlantic?

Significant advances in mapping structural and stratigraphic features in the Mundaú sub-basin are presented in this work. The possibility of finding the successful plays mapped in this work in other parts of the BEM, as well as in Equatorial Africa, is demonstrated in the following sections.

2. Geological setting

The Brazilian Equatorial Margin is associated with the opening of the Central Atlantic Ocean, itself formed by the fragmentation and continental breakup of northwest Gondwana during the Lower Cretaceous. At this time, a transtensional shear corridor with a dextral sense of movement was developed at the loci of the present-day north and northern continental margins of Brazil (Azevedo, 1991).

The BEM is characterised by the presence of east-west and northwest-southeast margin segments, forming *en echelon* structures that are typically associated with the predominant strike-slip tectonics of transform margins (Gorini, 1993). It includes, from east to west, the Potiguar, Ceará, Barreirinhas, Pará-Maranhão and Foz do Amazonas basins. The main characteristics of the BEM's offshore basins are: a) their relatively late continental breakup when compared to the Eastern Brazilian Margin (Françolin and Szatmari, 1987; Szatmari et al., 1987; Matos, 2000), b) a continental breakup stage controlled by strike-slip tectonics with predominant dextral kinematics (Matos, 2000; Basile et al., 2005), c) diachronous subsidence and uplift events on each margin segment controlled by divergent, transtensional or transpressional tectonics (Mohriak, 2003; Zalán, 2004), d) sub-basins that record contrasting histories in terms of their thermal, depositional, magmatic and deformation histories (Milani et al., 2000), and e) the absence of a transitional evaporitic sequence of Aptian age, as well as the absence of structures and sedimentation associated with salt tectonics (Mohriak, 2003; Zalán, 2004; Pellegrini and Severiano Ribeiro, 2018).

The Ceará Basin presents transpressional and transtensional segments and, because of its distinct tectonic character along and across the BEM, it has been previously divided into four distinct sub-basins (Morais Neto et al., 2003).

2.1. Ceará Basin

The Ceará Basin is bounded to the east by the Fortaleza High, to the west by the Tutóia High, to the south by crystalline basement, and to the north by the Romanche Fracture Zone (RFZ) (Costa et al., 1990) (Fig. 1). The basin has been divided into four distinct sub-basins, from east to west, each reflecting different structural styles: the Mundaú, Icaraí, Acaraú and Piauí-Camocim sub-basins (Morais Neto et al., 2003) (Fig. 1B). The Piauí-Camocim is separated from the Acaraú sub-basin by the Ceará High. The Acaraú and Icaraí sub-basins have, as common limit, the Sobral-Pedro II lineament. In addition, the Icaraí is separated from the Mundaú sub-basin by an important change in fault trends (Morais Neto et al., 2003). According to Matos (2000), deformation in the Mundaú sub-basin was essentially transtensional in nature, while the Piauí-Camocim sub-basin records one of the most important examples of transpressional deformation on the BEM, with compressive structures such as folds and thrust faults well developed there (Zalán and Warme, 1985).

Beltrami et al. (1994) suggested differences in the sedimentary record of the Mundaú, Icaraí-Acaraú and Piauí-Camocim sub-basins. The Piauí-Camocim sub-basin shows the less complete sedimentary fill of the three sub-basins, with unconformities and depositional hiatuses of greater magnitude. The most complete stratigraphic record is that of the Mundaú sub-basin (Fig. 2).

2.2. Mundaú sub-basin

The Mundaú sub-basin is a hydrocarbon-producing region with four oil and gas fields in its shallow waters: Xaréu, Atum, Curimã and Espada (Fig. 1). According to ANP (2020), this basin produces 4109 bbl/d of oil and 83 Mm^3/d of gas, totalling 4632 boe/d. Matos et al. (1996) demonstrated that faults delimiting the Mundaú sub-basin reveal significant changes in geometry, varying from 'planar' to 'listric', 'sigmoidal-listric' and 'listric with a flat-ramp profile'. In addition, they proposed three distinct architectures for the Mundaú sub-basin: 1) tilt blocks where the Mundaú Fault shows a planar or listric geometry at depth, 2) tilt blocks with a synclinal next to the Mundaú Fault due to its sigmoidal geometry, and 3) tilt blocks with anticlines and small synclines genetically related to the flat-ramp geometry of the Mundaú Fault. According to Antunes et al. (2008), the structural framework of the Mundaú sub-basin is dominated by a normal fault, the Mundaú Fault, which strikes NW-SE and dips to the NE (Fig. 1).

The tectono-sedimentary evolution of the Mundaú sub-basin consists of three major megasequences (Beltrami et al., 1994): syn-rift, transitional and drift. The syn-rift phase is characterised by the development of NW-SE normal faults bounding asymmetric half-grabens, and continental sedimentation marked by fluvial-deltaic sandstones and shales of the Mundaú Formation (Beltrami et al., 1994) (Fig. 2). The top of this unit is a regional stratigraphic horizon, called Electric Mark 100 (Costa et al., 1990) or 1000 (Condé et al., 2007), corresponding to a hard ground (Beltrami et al., 1994; Condé et al., 2007). It is interpreted as resulting from regional flooding affecting the basin during the lower Aptian (Pessoa Neto, 2004).

The transitional sequence (Paracuru Fm.) marks the first marine incursions affecting the Mundaú sub-basin, alternating within fluvial, deltaic and lacustrine sandstones. Limestones and subordinate evaporites were also deposited at this stage (Costa et al., 1990; Beltrami et al., 1994; Condé et al., 2007) (Fig. 2). As shown by Maia de Almeida et al. (2020), the Paracuru Formation represents a *breakup sequence* sensu Soares et al. (2012) and Alves and Cunha (2018).

The drift or marine megasequence, developed in association with

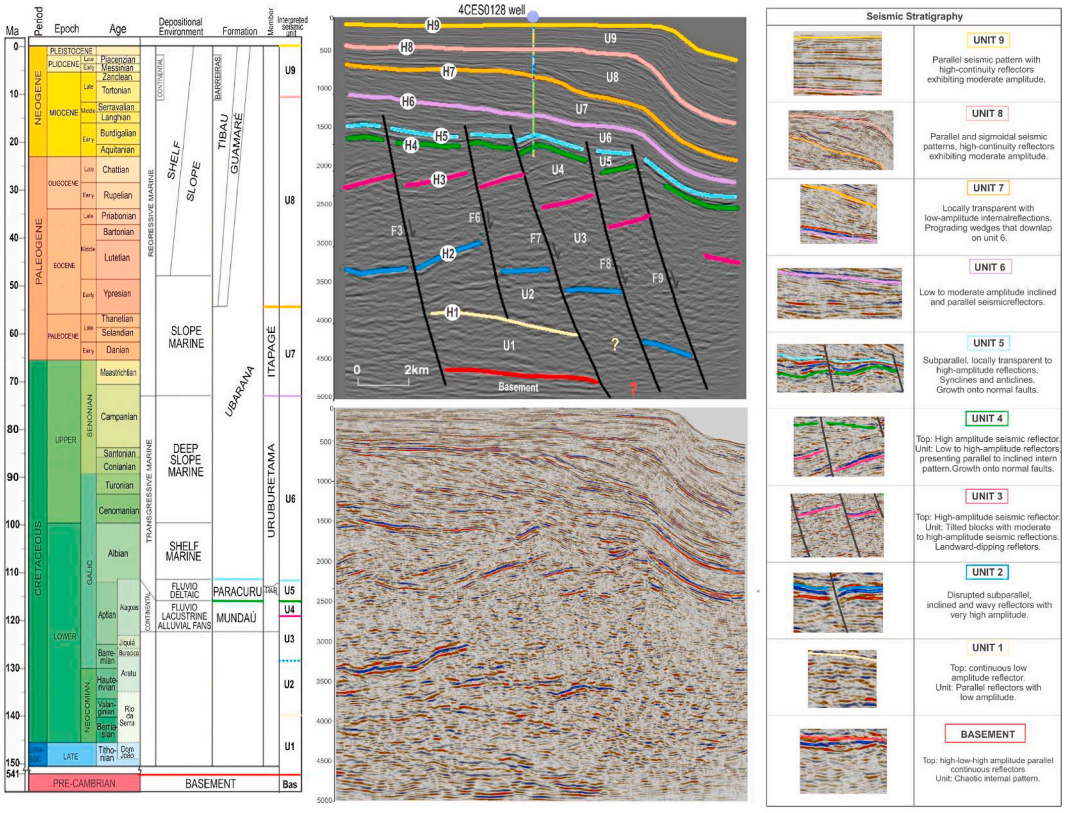

Fig. 2. Correlation panel showing the interpreted seismic units and detailed stratigraphic information from the Ceará Basin (Condé et al., 2007). See location of the seismic section in Fig. 1.

continental drift between the BEM and Equatorial Africa, reflects a prolonged phase of thermal subsidence. The resulting drift strata in the Ubarana Formation comprises two members (Costa et al., 1990; Beltrami et al., 1994; Condé et al., 2007) (Fig. 2). The first of these two members, the Uruburetama Member, corresponds to a marine transgression and consists chiefly of shales. The second member, the Itapagé Member, corresponds to a regressive marine phase and consists of turbiditic shales and sandstones (Costa et al., 1990; Beltrami et al., 1994; Condé et al., 2007). The Guamaré Formation consists of shelf carbonates, while the Tibau Formation comprises proximal sandstones. The clastic continental sediments of the Barreiras Formation are the youngest in the basin (Condé et al., 2007) (Fig. 2).

2.3. Curimã and Espada fields

The Curimã field is a classic example of a combined hydrocarbon trap resulting from the erosional truncation of large, active tilt blocks. This combined trap is made up of rotated blocks with Aptian strata truncated at the top by an angular unconformity, therefore juxtaposing Aptian reservoirs and Albian-Turonian transgressive shales (Pessoa Neto, 2004). The main reservoirs in the Curimã field comprise fluvial and deltaic sandstones with good permeability and porosity, strata that are laterally continuous in the Mundaú and Paracuru Formations. Porosity varies from 15.6% to 22.3% in the Paracuru Formation and 18.4%–27.7% in the Mundaú Formation, while permeability varies from 27.4 mD to 401.6 mD in the Paracuru Formation and from 65.2 mD to 212.8 mD in the Mundaú Formation (ANP, 2016). Reservoirs in the Paracuru Formation are filled with 31° API oil, whereas the Mundaú reservoirs contain 29°API oil. In the Paracuru Formation, the primary mechanism of production is gas in solution. In addition, water injection has been applied since 1985 with the aim of enhancing oil recovery. In the Mundaú Formation, the primary mechanism of production is combined water inflow due to an adjacent aquifer and resulting expansion of a gas cap (ANP, 2016).

The main reservoirs in the Espada field are located in a turbiditic play comprising sandstones intercalated with shales of the Ubarana Formation (Costa et al., 1990). The reservoirs are filled with 37° API oil (ANP, 2017a). The pay zone is approximately 10 m thick, where porosity varies from 24.5% to 32.3% and permeability varies from 200 mD to 9000 mD (ANP, 2013).

3. Material and methods

Data from 12 exploration wells and a post-stack time-migrated multichannel three-dimensional seismic reflection volume (0223_CURIMA_ESPADA_4 A.3D. MIG_FIN) were used in this study (Fig. 1). The interpreted seismic volume consists of 171 inlines spaced 75 m (IN95 – IN266) with a 35°azimuth, and 662 crosslines (XL77 - XL739) spaced 25 m with a 125°azimuth. It covers part of Espada field and the entire Curimã field, spanning the mid continental shelf, the outer continental shelf and the upper continental slope (Fig. 1). The inline length is ~16.6 km and crosslines are ~12.8 km long, reaching a total area of ~212 km^2. Penetration depth reaches 5000 ms two-way time (twt) and each seismic trace has 1251 samples at a 4 ms sampling interval. The 3D post-stack seismic data was supplied with a standard processing flow (migrated post-stack).

The interpreted well data include standard log suites (i.e. gamma ray, sonic, density and resistivity), lithological data and formation tops. Some wells (e.g. 4CES0128, 4CES0143 and 1CES0115) include check-shot surveys. All these data were acquired by Petrobras and supplied by the Brazilian National Agency of oil, gas and biofuels (ANP).

Well and seismic data integration was performed on Schlumberger's Petrel E&P Software Platform. The interpretation of the seismic data (horizons and faults) was performed in the time domain. Thus, we converted the well data into the time domain using the check-shots and sonic logs (Fig. 3). We produced a synthetic seismogram and correlated it to the real seismic data. Seismic interpretation was based on the general principles of seismic stratigraphy (Mitchum et al., 1977), which rely on the recognition of seismic patterns such as seismic terminations, seismic facies and seismic units. First, we interpreted the main seismic horizons and faults in the Mundaú sub-basin. In a second stage, we created fault polygons and their boundaries. Finally, horizon and fault interpretations were used to generate surfaces and then to compile the thickness maps (Fig. 3).

4. Results

4.1. Seismic stratigraphy

Nine seismic sequences were interpreted and correlated with the regional lithostratigraphic framework of Condé et al. (2007) (Figs. 2 and 4). Units 1, 2, 3 and 4 comprise the syn-rift Mundaú Formation.

The **top basement** reflection was mapped in the central part of the study area (Figs. 5j and 6). Here, basement rocks are characterised by their chaotic internal pattern, with the top of this unit comprising a continuous reflection of variable amplitude (Fig. 2). The top basement reflection generally dips to the NNW at an angle varying from 0° to 72°, with an average dip of 15°.

Unit 1 is characterised by its parallel internal reflections with low amplitude, similar to the basement, and was chiefly mapped in the central part of the study area (Figs. 5i and 6). The top of Unit 1 (Horizon 1) is a continuous low-amplitude reflection (Fig. 2).

The top reflection in **Unit 2** is a faulted, high-amplitude horizon that occurs at a depth of ~3000 ms two-way time (Horizon 2). Unit 2 is characterised by its sub-parallel, inclined and wavy internal reflections with very high amplitude (Fig. 2). A basement high affects the unit in the SSE part of the study area, where internal reflections dip to the NNW (Fig. 5h). Units 1 and 2 were not crossed by exploration wells.

The top of **Unit 3** (Horizon 3) is correlated with the Electric Mark 80 (Costa et al., 1990) or 800 (Condé et al., 2007). In the study area, this marker comprises a high-amplitude seismic reflection with poor continuity (Fig. 2). Horizon 3 is key to the mapping of faults when considered together with Horizon 2. Unit 3 shows moderate to high-amplitude seismic reflections tilted by normal faults. These reflections can be landward-dipping in places. Unit 3 is composed of intercalated shales and sandstones (Fig. 4) showing strata growth in the immediate footwall of normal faults (Fig. 7d). It reaches a maximum thickness of 1750 ms.

Unit 4 comprises low-to high-amplitude internal reflections that are horizontal to gently dipping. The unit is composed of sandstones, siltstones and shales (Figs. 2 and 4). Its upper boundary (Horizon 4) coincides with the high-amplitude Electric Mark 100 (Costa et al., 1990) or 1000 (Condé et al., 2007). Unit 4 fills multiple half-grabens and shows growth onto active faults, thus reflecting the development of a syn-rift sequence. In contrast to Unit 3, Unit 4 presents thicker strata on the downthrown side (immediate hanging-wall) of faults (Fig. 7c). All imaged faults intersect Unit 4 in its entirety (Figs. 5f and 6).

Unit 5 comprises sub-parallel, locally transparent to high-amplitude seismic reflections, part of the Paracuru Formation. It is composed of thin intercalations of sandstone, siltstone, shales and marls (Figs. 2 and 4). Unit 5 is a transitional unit, a *breakup sequence* sensu Soares et al. (2012) and caps the half-grabens associated with syn-rift faults. Its top (Horizon 5) is an angular unconformity; widespread erosion removed the upper part of this unit (Fig. 7b). As a result, Unit 5 becomes thinner in the east and southeast parts of the study area. To the east close to the 1CES0115 well, Unit 5 was totally eroded. Importantly, Units 4 and 5 grow onto major normal faults, revealing active tectonic subsidence during their deposition.

Unit 6 was deposited during the drift phase. However, faults still offset its lower part. Unit 6 displays low-to moderate-amplitude inclined reflections comprising calcareous shales with sandstones and siltstones intercalations (Fig. 4). Marls and calcilutites were drilled in some wells. Unit 6 comprises the Uruburetama Member of the Ubarana Formation

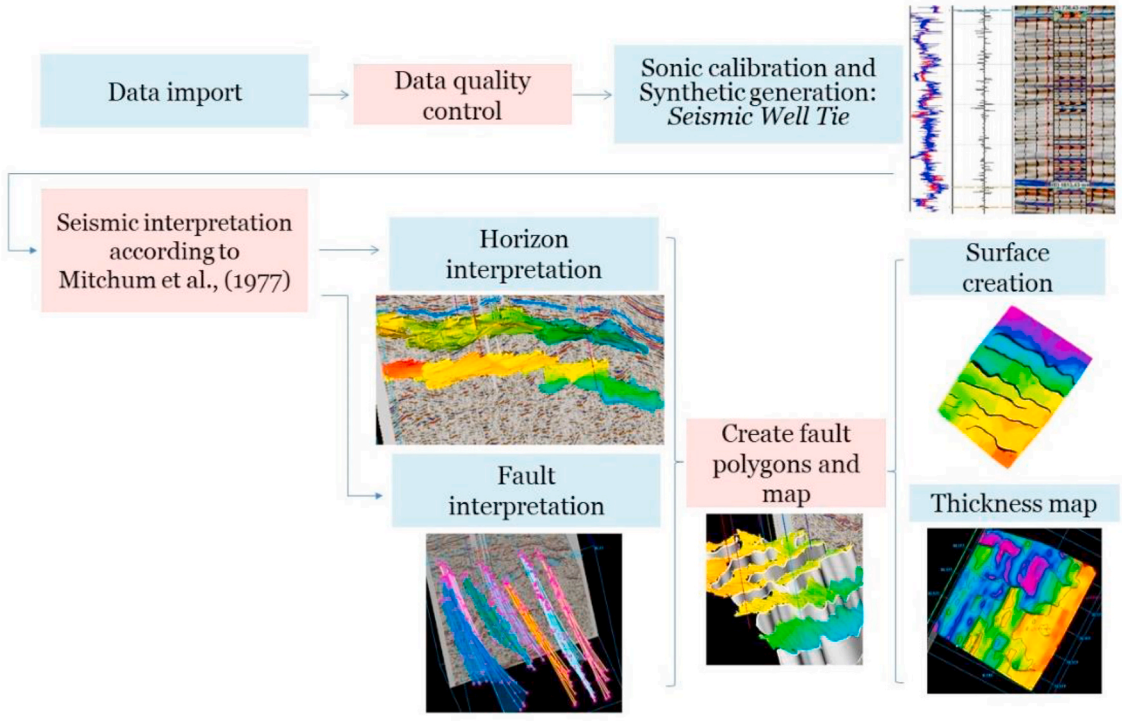

Fig. 3. Flow chart summarising the methodology used in this work.

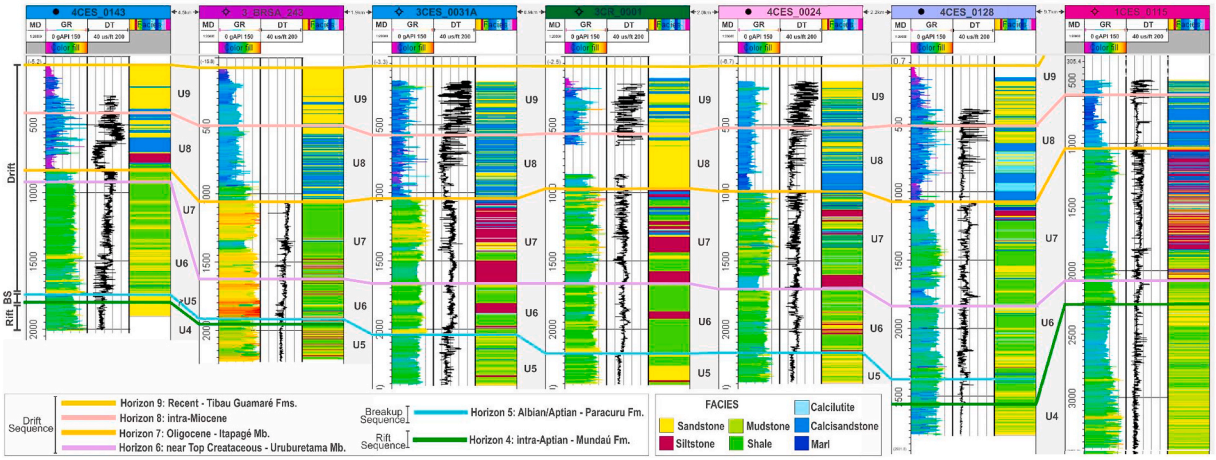

Fig. 4. Well correlation panel showing interpreted seismic units, gamma ray, sonic logs and facies. The panel also highlights the major sequences interpreted in this work: rift, transitional (breakup sequence) and drift.

(Fig. 2) and its top (Horizon 6) corresponds to an erosional surface associated with the incision of two submarine canyons. The Espada and Curimã fields are located between these two submarine canyons (Figs. 5d and 7a).

The upper boundary of **Unit 7** (Horizon 7) is a low-amplitude continuous reflector. Unit 7 is locally transparent with low-amplitude internal reflections (Fig. 2). In addition, Unit 7 reveals prograding wedges of strata that downlap onto Unit 6. Unit 7 comprises the regressive Itapajé Member of the Ubarana Formation; it is lithologically composed of intercalations of sandstones, siltstone, marls, calcilutites and shales (Fig. 4).

Unit 8 reveals parallel and sigmoidal seismic reflections with high continuity and moderate amplitude (Fig. 2). Lithologically, Unit 8 is composed of calcarenites, calcilutites, sandstones and shales (Fig. 4).

Unit 9 consists of parallel seismic reflections with high continuity and moderate amplitude (Fig. 2). It is mainly composed of sandstones and calcarenites with thin layers of shales. In the northern region of the study area there is a submarine canyon incising the continental shelf edge (Fig. 5a). Units 8 and 9 comprise the Tibau and Guamaré Formations.

4.2. Tectonic framework

The study area presents a synthetic arrangement to the main extensional fault bounding the Mundaú sub-basin (Mundaú Fault). In general, normal faults are seaward-dipping, strike to the NW, and are planar at depth (Figs. 2 and 6).

In the mid continental shelf, Faults 1, 2, 3 and 4 show an *en echelon* geometry (Figs. 5j and 6) and, except for Fault 4, offset basement units. Faults 2, 3 and 4 are respectively 2.7, 1.7 and 1.3 km long, being the

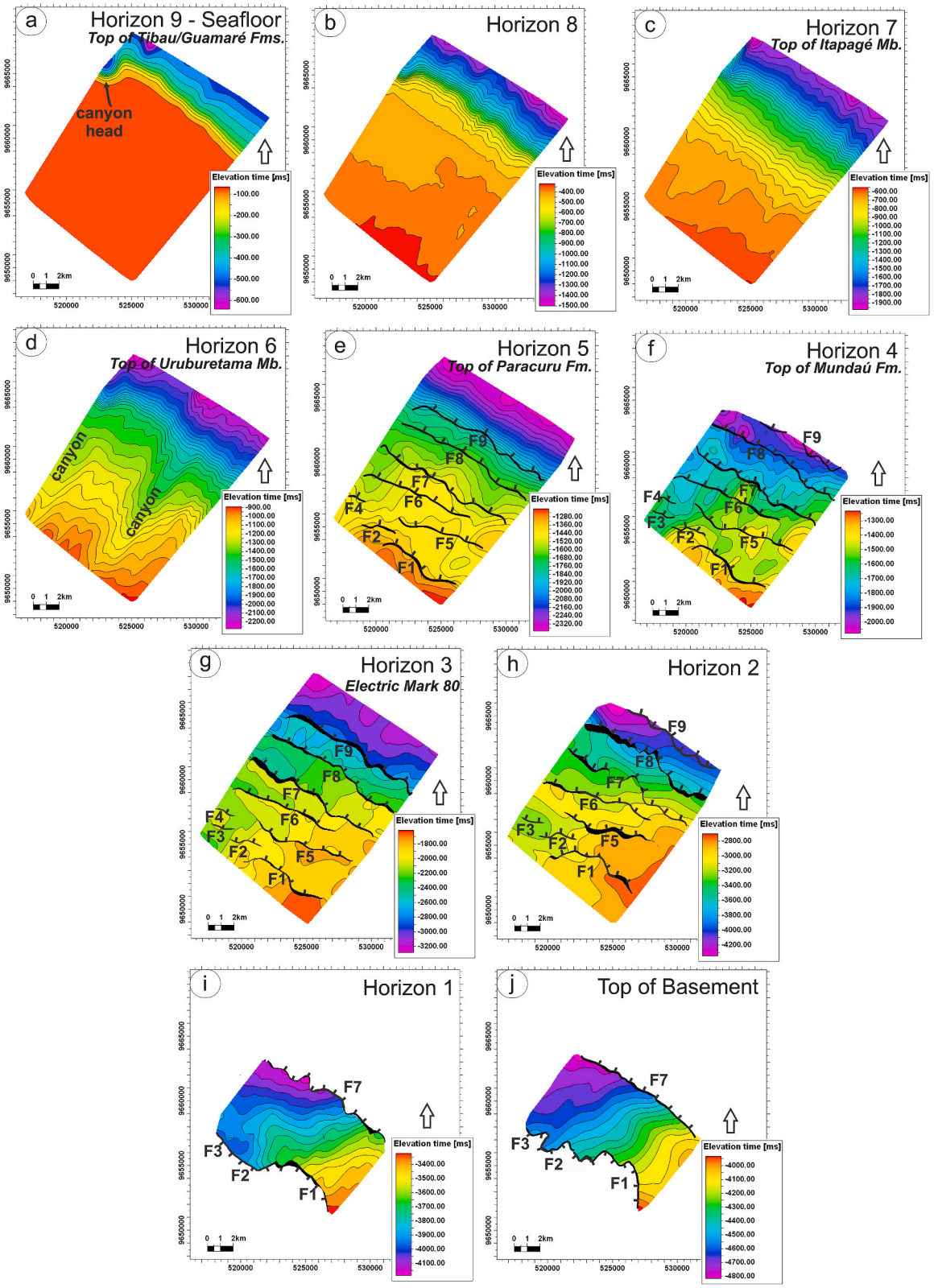

Fig. 5. Time-structural maps of various horizons in the study area: A) Sea floor (Top of the Tibau and Guamaré Formations) revealing submarine canyons in the shelf-edge region and on the continental slope. B) Horizon 8. C) Horizon 7 (Itapagé Member). D) Horizon 6, which corresponds to the top of the Uruburetama Member. Two submarine canyons incised the continental slope at this level. E) Horizon 5 (Top of the Paracuru Formation) revealing the reactivation of faults during the transitional phase. F) Horizon 4, correlating with the top to the Mundaú Formation. This horizon was offset the syn-rift faults. G) Mark 80 horizon (top of Unit 3). H) Horizon 2 showing a faulted surface with a structural high to the SSE. I) Top of Unit 1 (Horizon 1) as mapped in the central part of the study area. J) Top of Basement mapped in the central part of the study area.

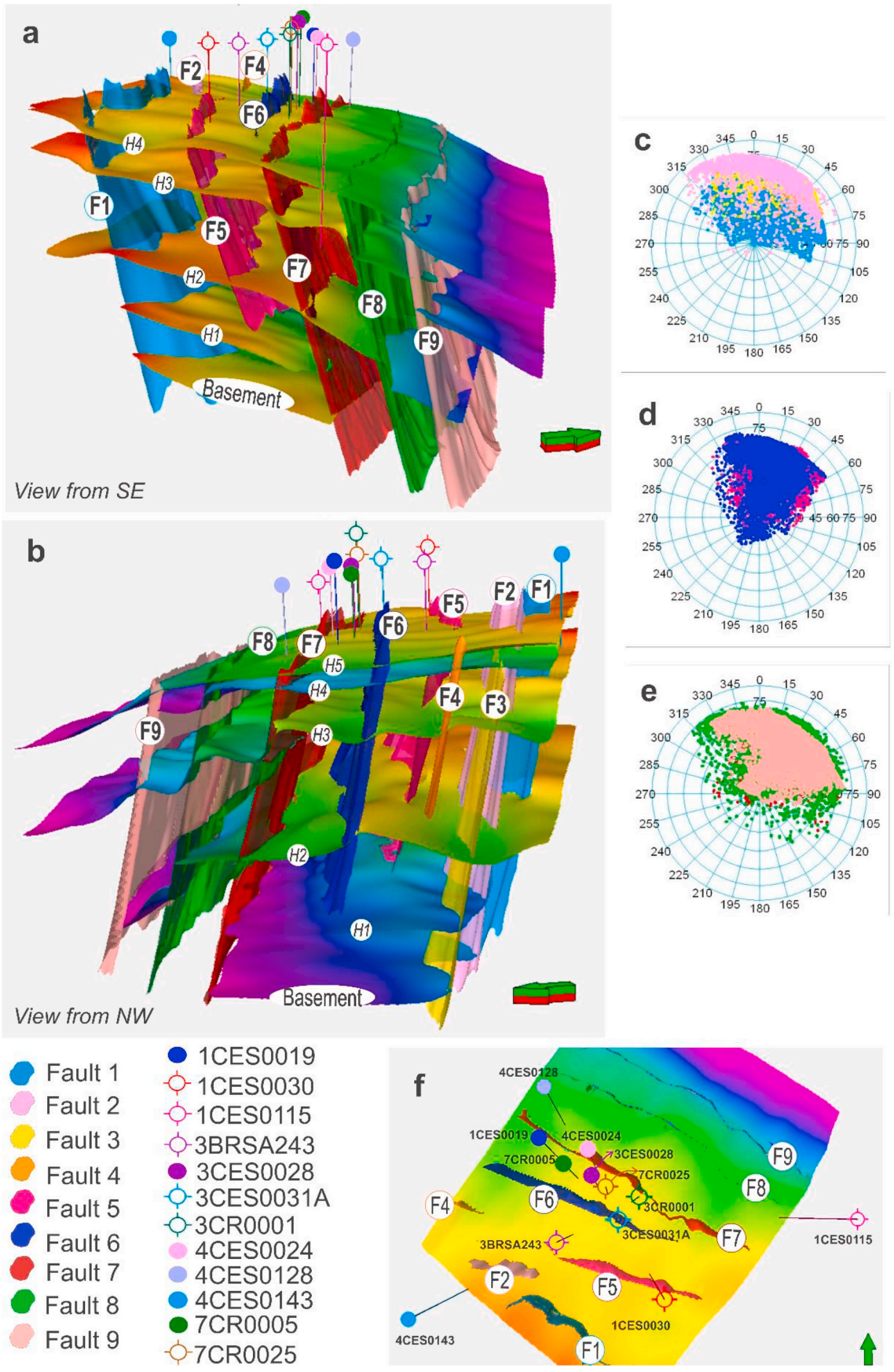

Fig. 6. A) and B) 3D structural models of the study area with views from southeast and northwest, respectively. C) Stereoplot of interpreted fault planes (as interpreted from seismic) showing the dip angle and dip azimuth of Faults 1, 2, 3 and 4. D) Corresponding stereoplot for Faults 5 and 6. E) Corresponding stereoplot for Faults 7, 8 and 9. F) Map view from above showing interpreted faults 1 to 9 and exploration wells.

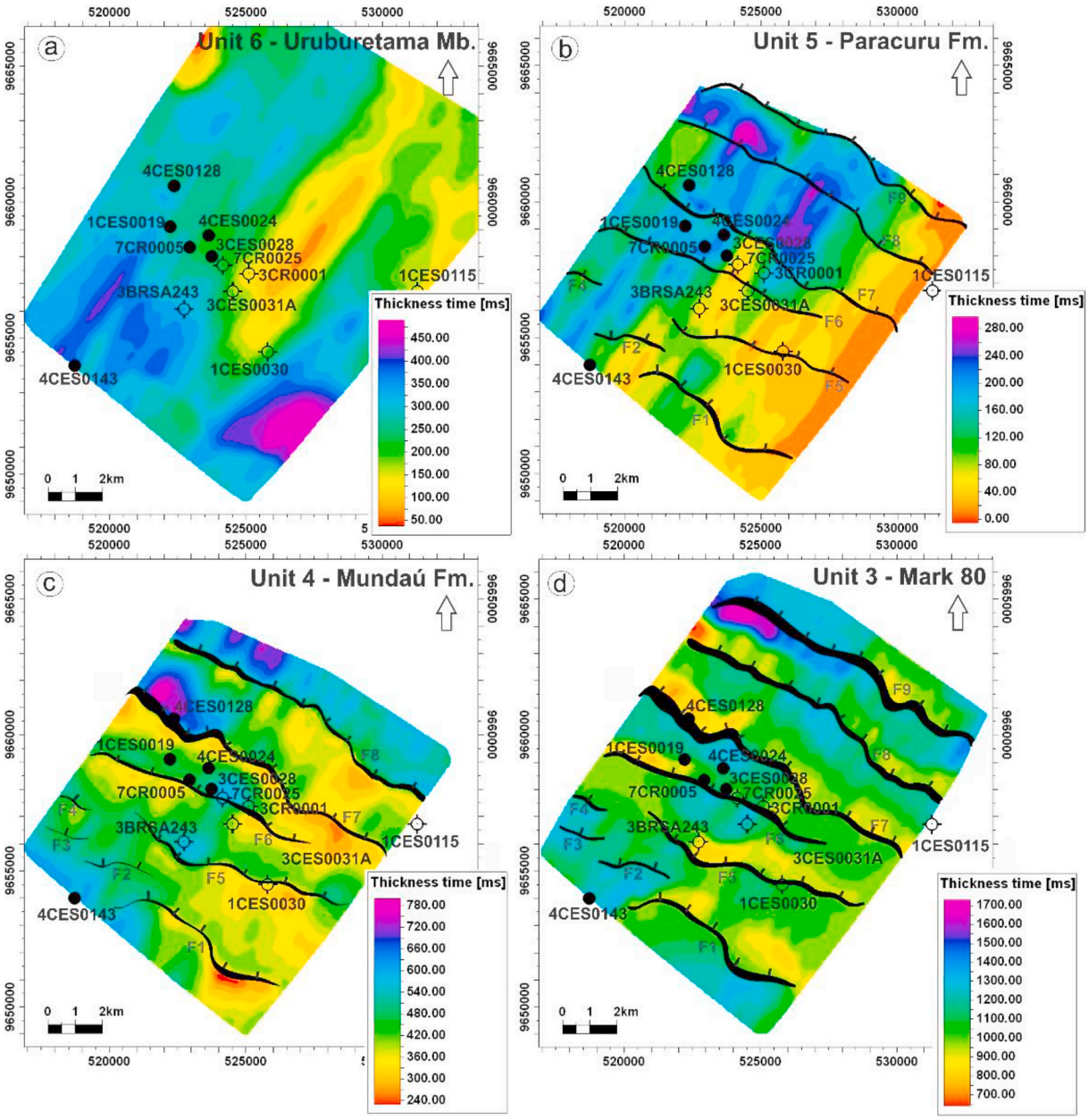

Fig. 7. Isochron thickness of: A) Unit 6 (Uruburetama Member). In the central part of the study area, there is a region with smaller thickness - see orange color. B) Unit 5 (Paracuru Formation). Widespread erosion removed the upper part of this formation reducing its thickness in the south and southeast of the study area. C) Unit 4, corresponding to the upper part of the Mundaú Formation. This map shows the sedimentary thickening on the downthrown side of faults, proving fault activity. D) Unit 3, showing an increase in thickness as one gets closer to the upthrown side of normal faults. (For interpretation of the references to color in this figure legend, the reader is referred to the Web version of this article.)

smallest faults in the study area. They are closely spaced with an average spacing of around 1 km, and with relatively rectilinear traces. This is chiefly the case for Faults 3 and 4 (Figs. 5 and 6).

Faults 5 and 6 present sinuous traces and offset Units 2 to 6, tipping out near the top of Unit 1 (Fig. 6). Faults are up to 9 km long and dip to the NNE with and average angle of 41° (Fig. 5).

On the outer shelf, the high-angle Faults 7, 8 and 9 are the longest in the study area (~11 km), occurring along the entire seismic volume. Fault 7 is located 2.7 km away from Fault 8, while this latter is spaced 1.9 km from Fault 9. All these faults are parallel and sinuous. Furthermore, they are responsible for the largest offsets observed in the study area.

4.3. Well data from the Curimã and Espada fields

After completing detailed seismic and structural interpretations, one can understand that wells 1CES0019, 4CES0024, 3CES0028 and 7CR0005 were drilled between Faults 6 and 7, successfully striking oil in the Curimã field (Table 1, Figs. 6 and 7). Wells 3CR0001 and 7CR0025 were also drilled between Faults 6 and 7, but did not find any hydrocarbons.

Well 4CES0128, drilled between Faults 7 and 8, found new reservoir intervals in the study area (Table 1, Fig. 8a). Fault activity resulted in the formation of an anticlinal trap near Unit 5, i.e. in the Paracuru Formation. Well 4CES0128 found oil in Units 4, 5 and 6 (Ubarana, Paracuru and Mundaú Formations).

In the eastern part of the study area, where the basement is shallow

Table 1
Integrated compilation of data from exploration wells and seismic interpretation, showing the well location between the interpreted faults, oil field names, category, aim, classification and oil finds.

Well	Drilled between the faults	Oil field	Year	Category	Aim	Classification	Oil finds
1CES0019	6 and 7	Curimã	1978	Pioneer	Testing of the dome structure next to the Paracuru top. Target: reservoirs of Paracuru and Mundaú Fms.	Discoverer of oil field	Units 5 and 6
4CES0024	6 and 7	Curimã	1978	Adjacent pioneer	Main target: sandstones in the Paracuru Fm. equivalent to sands in the 1CES0019 producer well. Secondary target: Turbiditic sandstones in the Ubarana Fm.	Subcomercial oil producer	Units 4, 5 and 6
3CES0028	6 and 7	Curimã	1978	Extension	To verify the SE extension of oil trapped in the Curimã field	Oil producer	Unit 5
7CR0005	6 and 7	Curimã		Exploration well	To investigate reservoir parameters and static pressure level	Comercial oil producer	Unit 5
4CES0128	7 and 8	Curimã	1996	Adjacent pioneer	To test the dome structure next to the Paracuru top	Discoverer of new oil area	Units 4, 5 and 6
3CR0001	6 and 7	Curimã	1979	Extension	To verifying the SE extension of oil trapped in the Curimã field	Dry with oil shows	–
7CR00025	6 and 7	Curimã	1989	Exploration well	To investigate reservoir parameters and static pressure level	Dry with oil shows	–
3CES0031A	5 and 6	Curimã	1979	Extension	To verify the SE extension of oil trapped in the Curimã field	Dry	–
3BRSA243	5 and 6	Curimã	2003	Extension	To verifying the S extension of oil trapped in the Curimã field	Dry	–
1CES0030	5 and 6	–	1979	Pioneer	To test the tilt block formed by fault 5	Dry	–
1CES0115	7 and 8	–	1991	Pioneer	To test the tilt block structured between faults 7 and 8	Dry with oil shows	–
4CES0143	2	Espada	1998	Adjacent pioneer	To drill turbiditic sandstones in the Ubarana Fm.	Subcomercial oil producer	Unit 6

and Unit 5 was eroded, well 1CES0115 was drilled with the aim of testing the half-graben delimited by Faults 7 and 8 (Fig. 7). The well crossed fluvio-deltaic sandstones in Units 3 and 4 (Figs. 4 and 6). However, this same well revealed reduced net pays, an undefined oil water contact, low transmissibility and very low productivity. The section below Horizon 3 showed very poor reservoir quality with a marked reduction in porosity with depth – a character further worsening the quality of the reservoirs drilled at this location. The well was classified as 'dry with hydrocarbon shows' and was abandoned.

Well 3CES0031A was drilled on top of the footwall bounded by Fault 6. This and well 3BRSA243 were drilled between Faults 5 and 6 with the aim of verifying the SE extension of the Curimã field (Figs. 6 and 7, Table 1). They did not find any hydrocarbons and were considered dry.

Well 1CES0030 was drilled exactly at Fault 5, reaching the lower part of the block limited by Faults 5 and 6, i.e. the immediate hanging-wall of Fault 5 (Fig. 8b). Well data show clayey sandstones, water saturation and low permeability. The well was eventually abandoned due to the lack of economic volumes of hydrocarbons. Well 1CES0143, in the southwest portion of the study area, is located in the Espada field (Table 1, Figs. 1 and 6). It detected oil shows in Units 5 and 6 and is, at present, an oil producer within the Ubarana Formation. Well tests developed in the interval spanning 1263–1278 m produced 26°API oil with a flow of 80 m^3/day (Fig. 8d).

5. Discussion

5.1. 3D structural modelling of an oil producing region of the BEM

Our 3D structural modelling suggests that the study area, comprising an oblique rift basin with multiple half-grabens, records active faulting during the deposition of Units 1 to 4 (syn-rift). Fig. 7c and d shows that important fault activity occurred during the deposition of Unit 4 (Aptian). These faults were capable of tilting the blocks where Units 2 and 3 were deposited (Fig. 7d), resulting in the thickening of Unit 4 next to fault planes (growth faults) (Fig. 7c). These observations corroborate the published literature and confirm that the continental margins along the Equatorial Rift Segment (EqRS) were affected by a paroxysmal phase of tectonism between South America and Africa during the Aptian, with a major phase of rift-related subsidence being reported from all EqRS basins (Azevedo, 1991; Brownfield and Charpentier, 2006; Soares Júnior et al., 2011; Heine and Brune, 2014).

Near the Xaréu Oil Field (Fig. 1), Antunes et al. (2008) mapped an array of NW-trending and NE-dipping normal faults forming an extensional system that is very similar to the study area in this work. However, faults in the Xaréu field are listric and rooted along a detachment surface corresponding to the Mundaú Fault, located at the southwest border of the Mundaú sub-basin. In addition, Antunes et al. (2008) interpreted these faults as representing listric or ramp-flat-ramp geometries. According to the interpretations in this work, faults are planar and sub-vertical in the Curimã field, forming tilt blocks. This compares favourably with basins on the BEM (Watts et al., 2009; Zalán, 2015) and Equatorial Africa (Tetteh, 2016) such as in the Guyana–Suriname (Nemčok et al., 2016a, 2016b), in which syn-rift planar faults were also recognised.

During the deposition of Unit 5 (transitional unit), faults continued to be active as transtensional structures, forming fold traps between active faults (Fig. 8a, c, 9e and 9f). The top of Unit 5 is an erosional unconformity recognised in the western portion of the Equatorial South America (Nemčok et al., 2016a), as well as in Equatorial Africa (Brownfield and Charpentier, 2006), and has been interpreted as a breakup unconformity. The exact location along the EqRS where continental breaup was occurring at the time, or if this stratigraphic surface represents full lithospheric or mantle breakup, is still under debate (see Soares et al., 2012; Alves and Cunha, 2018; Maia de Almeida et al., 2020). Similarly to the study area, Nemčok et al. (2016a, 2016c) show evidence for folding of strata near the breakup unconformity before late Aptian–Albian times. They noted the presence of the breakup unconformity on top of a folded section characterised by significant erosion of the Demerara Plateau. In parallel, Attoh et al. (2004) confirmed that this same episode is associated with subaerial erosion offshore Ghana, and attributed lateral variations in erosional depth to crustal displacement associated with local folding and uplift.

The development of folds in extensional basins is not common; however, fault-related folds have been recognised close to propagating normal faults (Brandes and Tanner, 2014), similarly to what is observed in the study area (Figs. 8 and 9). Fault-related folding has been analysed in the field (Howard and John, 1997; Corfield and Sharp, 2000; Sharp et al., 2000), using analogue models (Withjack et al., 1990), and numerical simulations (Khalil and McClay, 2002; Jin and Groshong, 2006). Analogue models developed by Mcclay and Scott (1991) reveal that small irregularities in the geometry of normal faults can generate reverse secondary faults and local antiforms within a general setting dominated by regional extension. These antiforms are similar to the structure drilled by well 4CES0128 (Fig. 8a).

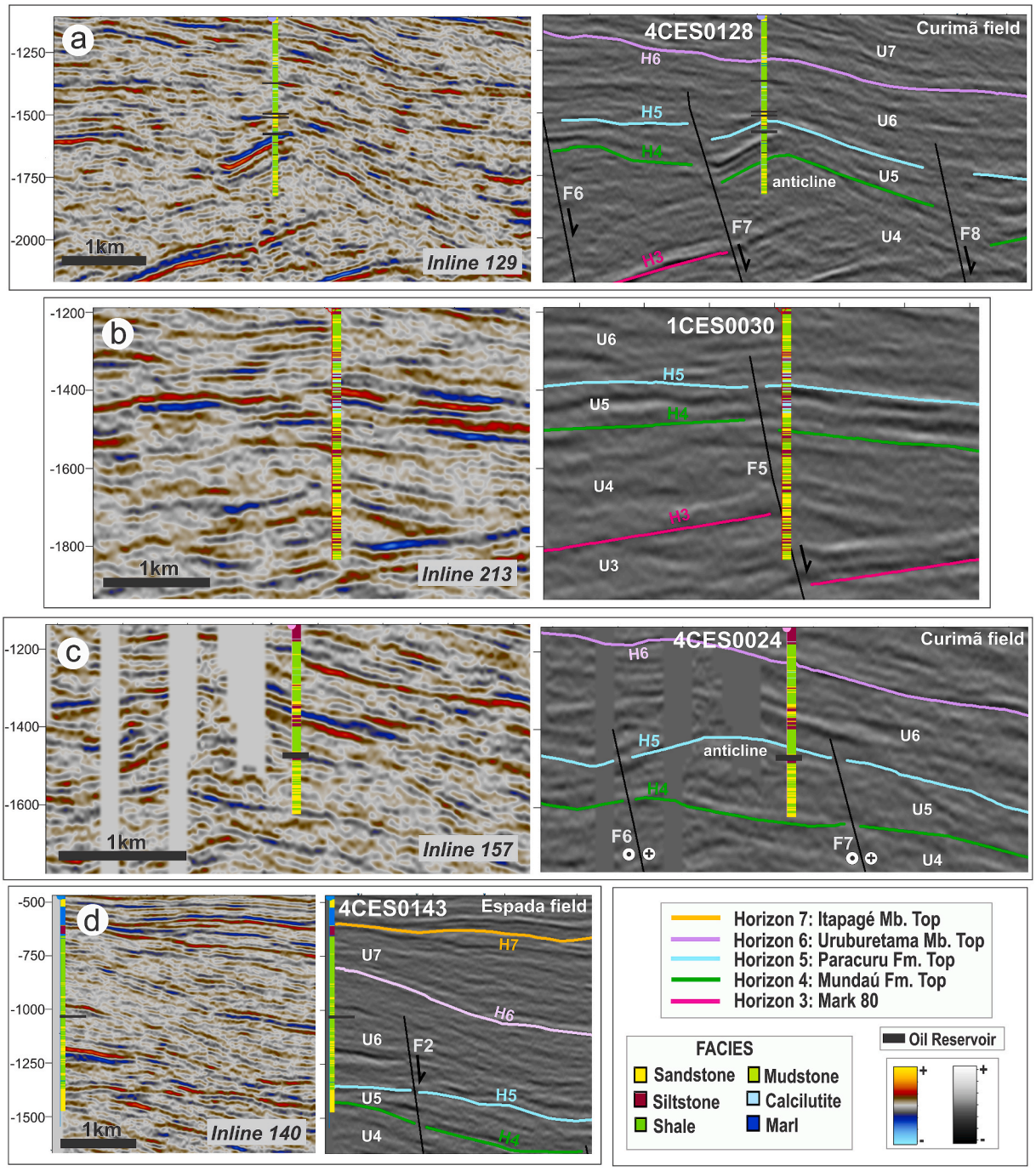

Fig. 8. Interpreted SW-NE seismic sections with faults, horizons and wells highlighting main seismic units in the study area. A) Well 4CES0128 reached Unit 4 (Mundaú Fm.) and drilled oil reservoirs in stratigraphic (turbiditic) and structural (anticline) plays. B) Well 1CES0030 drilled in the fault zone (downthrown side of Fault 5). C) Well 4CES0024 drilled on the immediate footwall of the Curimã Fault (Fault 7). Anticline structure on the tilt-block formed between Faults 6 and 7 at the level of Unit 5 (Paracuru Formation). This anticline shows an accumulation of oil in place. D) Well 4CES0143 crossing the Espada field and corresponding turbiditic reservoir successions in Unit 6 (Ubarana Formation).

Folds generated between normal faults can also be associated to strike-slip tectonics (Zalán, 1986; Lamarche et al., 1997; Davison et al., 2016). According to Fossen et al. (2013) and Fossen (2016), transcurrent faults zones can develop folds; folds are arranged spatially such that culminations and depressions in successive folds lie along lines that make an acute angle with the (approximately parallel) fold axes. Such folds are stepped, and, in general, arranged in an *en echelon* geometry. In the study area, folds are relatively sub-parallel to faults, showing very acute angles. In addition, folds were mapped in other regions of the BEM such as in Barreirinhas and Pará-Maranhão basins by Azevedo (1991) and Sauerbronn (1996), in the Piauí-Camocim sub-basin by Zalán and Warme (1985), in the Icaraí sub-basin by Castro (1993), in the Potiguar Basin by Hoerlle et al. (2007), in the Guyanas-Suriname basins by Goss et al. (2008), Nemčok et al. (2016a) and Loncke et al. (2016) and in Equatorial Africa by Attoh et al. (2004), Lamarche et al. (1997) and Davison et al. (2016).

The *en echelon* geometry of normal faults observed in the study area is a common character in transcurrent structures (Hempton and Neher, 1986; Deng et al., 1986; Lonsdale, 1989; Moustafa and Abd-Allah, 1992; Zachariasen and Sieh, 1995) (Figs. 5 and 7). Hence, using the criteria of

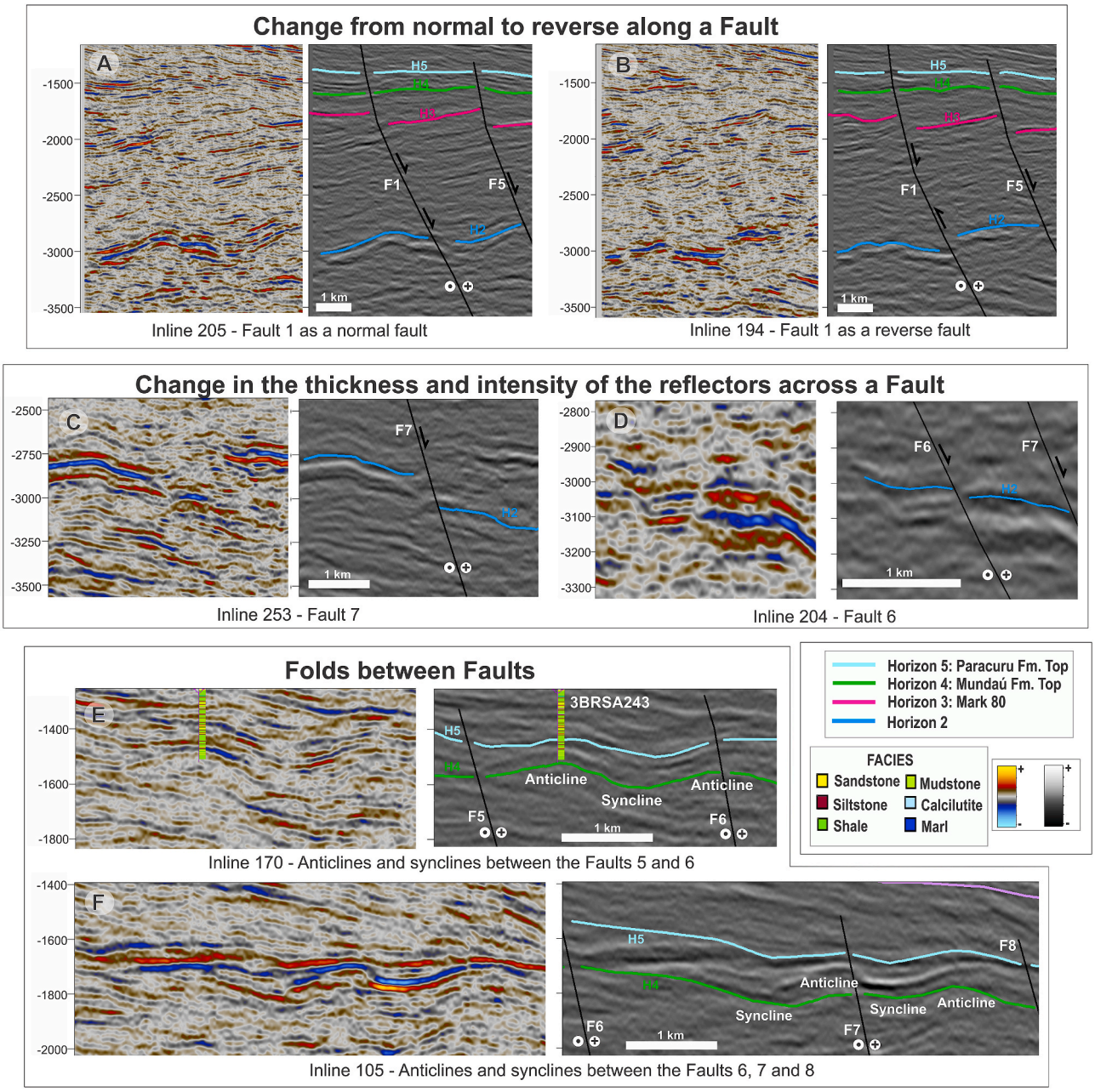

Fig. 9. Seismic geometries of strike-slip tectonics. A) Variations of fault throw with depth (Fault 1). B) Change from normal to reverse fault movement with depth (Fault 1). C) Abrupt change in the seismic character of seismic reflectors crossed by Fault 7. D) Abrupt change in the seismic character of seismic reflectors crossed by Fault 6. E) Synclines and anticlines in the breakup sequence (Unit 5) between the faults 5 and 6. F) Synclines and anticlines in the breakup sequence (Unit 5) between the faults 6, 7 and 8.

Zalán (1986), other characteristics revealing strike-slip movements were investigated in the study area, such as the sinuous and complex geometries of fault planes and profiles (Figs. 6 and 7). High sinuosity in faults is an important trait of transcurrent faults (Bridwell, 1975). Moreover, Fault 1 changes from normal to reverse along its strike (Fig. 9a and b). In Fig. 9a, Horizons 2 and 3 are subtly displaced by Fault 1. However, in Fig. 9b, Fault 1 displaced Horizon 2 as a reverse fault and Horizon 3 as a normal fault. Apart from changing from normal to reverse fault along strike, this fault also reveals important changes in throw with depth, two characteristics associated with strike-slip movements (Zalán, 1986). Offshore Ghana, Attoh et al. (2004) also mapped contradictory offsets that indicate strike-slip tectonics.

Variations in the seismic character across a fault were also interpreted as relating to strike-slip movements in our seismic data. Seismic facies reveal changes in thickness and intensity of the seismic reflections, and relative scale of deformation in strata (Fig. 9c and d), corroborating the idea that strike-slip tectonics affected great part of the study area. Similarly, Andrade et al. (2018) interpreted changes in the seismic reflections close to the Romanche Fracture Zone as revealing a dense set of strike-slip faults. Such interpretations have important economic implications because it increases the variability of potential traps around the Romanche Fracture Zone (Zalán, 1986).

Ultimately, the 3D structural model presented in this work is a combination of Geometries 1 and 3 proposed by Matos et al. (1996) (*see item 2.1.1 Mundaú sub-basin*). Therefore, we propose a fourth complementary geometry that includes tilted blocks with small anticlines and synclines genetically related to transtensional planar faults. This model fits within the regional context of oblique rifting in the Brazilian

Equatorial Margin.

5.2. Petroleum plays in the Curimã and Espada fields: comparison with other Equatorial Atlantic plays

Three types of petroleum plays were found in the study area: combined, structural and stratigraphic (Fig. 10). They are described as follows:

5.2.1. Combined plays

Pessoa Neto (2004) summarised the essential conditions to form combined traps in the Curimã field: large-slip faults and the presence of angular unconformities followed by the deposition of thick transgressive marine shales. In addition, three geological settings were considered by Pessoa Neto (2004) to record some degree of inefficiency in hydrocarbon traps: 1. juxtaposition of reservoir intervals and sandy layers across fault planes or unconformities; 2. the absence of erosional truncation in tilt blocks and; 3. erosion or non-deposition of transgressive marine strata above reservoir intervals.

Based on our 3D structural model, Faults 6 and 7 are key to understand the petroleum potential of the Mundaú sub-basin - wells 1CES0019, 4CES0024, 3CES0028 and 7CR0005 drilled between these two faults and found oil in the Curimã field (Table 1, Figs. 7, 8 and 10). These wells drilled key examples of the **combined plays** proposed by Pessoa Neto (2004). Wells 1CES0019 and 4CES0024 reached a dome structure formed by Faults 6 and 7 and reached the upthrown side (footwall) of a mixed trap formed by the block tilted by Fault 7 and the shales deposited above Horizon 5 (Figs. 8c and 10). The upthrown sides of normal faults, forming tilt blocks, are classic footwall traps for hydrocarbon (Illing and Hobson, 1981; Brooks and Glennie, 1987; Yielding, 1990; Hardman and Booth, 1991; Nemčok, 2016). According to Pessoa Neto (2004), Aptian reservoirs are located on the footwall of the main fault bounding the Curimã field, i.e. the Curimã Fault. Thus, we can deduce that Fault 7 is the Curimã Fault proposed by Pessoa Neto (2004).

The Curimã field is delimited to the north by the Curimã Fault (Fault 7), which affects Units 4 and 5 (Paracuru and Mundaú Formations). However, Fault 7 also offsets the lower part of Unit 6 (Uruburetama Member). To the south, the field is delimited by a synthetic normal fault (Fault 6). Similarly to the Curimã field, there are hydrocarbon accumulations in deep-water Ceará (Pecém discovery) and Potiguar Basins (Pitu discovery) that show combined plays, as presented by Maia de Almeida et al. (2020) and ANP (2017b). Aptian transitional reservoirs were trapped by a normal fault and an erosional unconformity. The Espoir and Baobab fields in Ivory Coast are also trapped by faulted blocks and the Albian unconformity (Kelly and Doust, 2016). These authors explained that reactivation of the inherited rift structures helped forming combined structural and stratigraphic traps.

The Jubilee Field in Ghana comprises a combination of structural and stratigraphic traps associated with the topography created by the transform tectonics during the opening of the Atlantic (Dailly et al., 2017). It is an Upper Cretaceous high-quality oil pay (Turonian in age) within a drift submarine fan sequence. In the Mundaú sub-basin, the combined plays occur in the Aptian transitional sequence. Nevertheless, the presence of more recent combined plays such as those at Jubilee cannot be ruled out in the Mundaú sub-basin as suggested by Maia de Almeida et al. (2020) and Leopoldino Oliveira et al. (2020), as well as in other basins of the Equatorial Atlantic exemplified by the Zaedyus field in French Guiana, considered an analogous example of the African Jubilee field.

5.2.2. Structural plays

Well 4CES0128 was classified as a new discovery between the Curimã Fault and Fault 8 (Table 1, Figs. 8a and 10). The Curimã Fault was capable of forming hanging-wall blocks with broad anticline traps as the one reached by this well, i.e. a **structural play**. Close to well 4CES0128, the Curimã Fault shows a relatively large offset, and Fig. 7a shows the deposition of Uruburetama shales. This well proved that hanging-wall block and anticline traps can be successful targets in the Mundaú sub-basin.

Jianping et al. (2010) presented different kinds of traps developed in tectonically-controlled strata along the Côte d'Ivoire-Ghana transform margin. They showed that most traps are structural, chiefly fault-block and anticline traps. They interpreted that anticline traps are related to the transform structures at the end of the St. Paul and Romanche Fracture Zones.

5.2.3. Stratigraphic plays

The Espada field, crossed by well 4CES0143, comprises a **stratigraphic play** composed of Upper Cretaceous turbiditic reservoirs occurring between 1262 and 1278 m (~1030 ms in the interpreted seismic volume). These reservoirs are located close to Faults 1 and 2 (Figs. 8d and 10). These faults do not trap oil; instead, they are related to the migration of oil into the Espada field. Such an interpretation takes into account that oil accumulated in the Ubarana Formation was generated in the Paracuru Formation and used faults as migration paths to turbidite sands in the Espada field (Costa et al., 1990). In addition, well 4CES0128 also reached Upper Cretaceous pinched-out turbiditic sandstones forming a stratigraphic trap (Figs. 8a and 10).

Recent (and important) discoveries have drawn the attention to these subtle stratigraphic traps (Dolson et al., 2018; Ward et al., 2016, 2018). As an example, the Stabroek block in Guyana includes several fields such as Liza, Payara, Liza deep, Snoek, Turbot, Pacora and Mako fields. This block contains sediments of Amazonian origin, which were deposited by the Guiana Current. There are multiple play types in this block, including Cretaceous and amplitude-supported plays containing stratigraphic onlaps, turbidites and basin floor fans (Offshore, 2020; Zhang et al., 2019). According to Zalán et al. (2019), the trapping mechanism

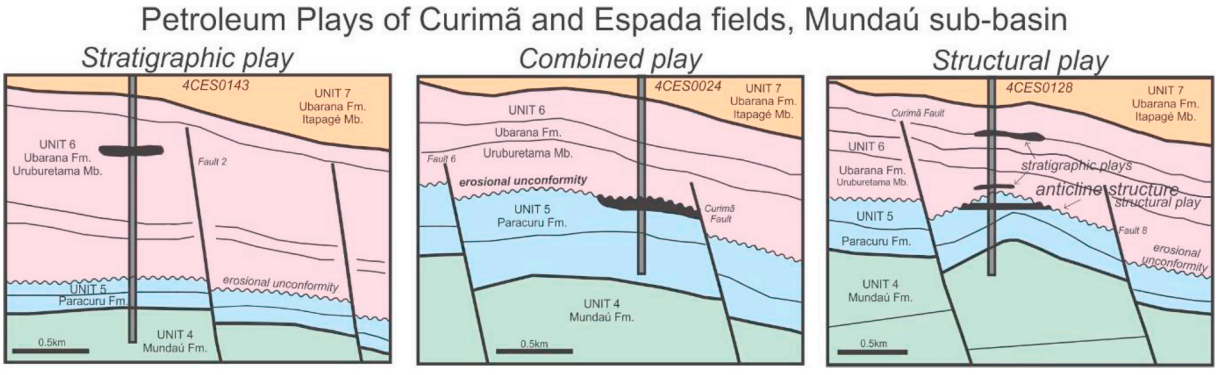

Fig. 10. Three types of petroleum plays in the Curimã and Espada fields, Mundaú sub-basin: stratigraphic, combined and structural plays.

in deep and ultra-deep waters of the Equatorial Atlantic is invariably stratigraphic in nature, with lateral and updip pinch outs limiting the reservoirs containing hydrocarbons. These authors are hopeful to replicate this success in the Foz do Amazonas and Pará-Maranhão Basins.

In the BEM, Pelegrini and Severiano Ribeiro (2018) mapped turbiditic plays in depositional pinch-outs (sandstones inside shales) in shallow and deep waters off Pará-Maranhão. In deep-water Mundaú sub-basin, stratigraphic traps were created by depositional pinch-outs and by volcanic bodies - turbiditic sandstones were interpreted as having reflectors with high acoustic impedance contrasts, low frequency, lensoid geometry, and variable lateral extension, ranging from 5 to 8 km (Leopoldino Oliveira et al., 2020).

Finally, the recent discoveries of the Pelican and Rossignol wells confirm that Upper Cretaceous stratigraphic plays in the deep-water Tano Basin (Ghana) comprise prolific reservoir intervals (Scarselli et al., 2018). Dailly et al. (2013) also concluded about the importance of stratigraphic plays in the Gulf of Guinea. Thus, the results presented here show successful plays of Mundaú sub-basin that can be replicated in other parts of the Equatorial South Atlantic, as well as in Equatorial Africa.

5.3. Exploration failures in the mundaú sub-basin

Unfortunately, some cases of exploration failures were recorded in the study area. For example, wells 3CR0001 and 7CR0025 drilled strata between Faults 6 and 7 but failed to find any hydrocarbons (Table 1 and Fig. 6). This means that a putative extension of the Curimã field to the southeast cannot be confirmed due to the smaller thickness of Units 5 and 6 in this region (Fig. 7a and b). The relatively minor thickness of Unit 5 can be related to widespread erosion during the Aptian-Albian (Morais Neto et al., 2003; Condé et al., 2007; Brownfield and Charpentier, 2006; Nemčok et al., 2016a), which removed part of this formation in the east and southeast parts of the study area. In contrast, the observed thinning of Unit 6 can be attributed to an erosional event of regional expression affecting Maastrichtian strata (Morais Neto et al., 2003).

Well 1CES0115 was drilled between Faults 7 and 8, similarly to the successful well 4CES0128. However, due to the presence of a structural high in the east and southeast, Unit 5 was totally eroded close to well 1CES0115 (Figs. 5 and 7b). Although oil shows were found in Unit 4, reservoir quality was poor. This well confirmed that basement faults controlled deposition during the syn-rift and transitional stages, and that basinwide erosional events contributed to the removal of prolific reservoir intervals in Unit 5.

Wells 3BRSA243 and 3CES0031A were drilled between Faults 5 and 6 with the aim of verifying the southeast extension of the Curimã field. Yet, they were considered dry (Table 1) and, based on the data in this work, we can infer that Fault 5 does not form a competent seal. It is worth pointing out that transcurrent faults change their properties along strike (Zalán, 1986). Well 3CES0031A was drilled in a region showing erosion of both Units 5 and 6 (Fig. 7), further decreasing its chance for success.

Well 1CES0030 was considered a wildcat; the aim was to test the footwall of the Fault 5. Nevertheless, this well reached its fault zone, crossing Unit 5 on the hanging-wall block and the Electric Mark 80 on the footwall (Fig. 8b). This well crossed clayey sandstones of low permeability, with cataclasites in the fault zone reducing their grain size, porosity and permeability. Clay minerals formed in the fault zone tend to compromise reservoir quality. Furthermore, this well was drilled on the margin of a submarine channel incising Unit 6, the main seal interval in the study area, a detail that may have led to the failure of well 1CES0030 as a wildcat.

This work correlated data with very different resolutions, e.g. seismic data (3D) with a resolution of hundreds of meters and well data (1D) with a resolution of dozens of centimeters. The different scales of seismic and well data do not permit a coherent assessment of reservoir lateral continuity, considering that the main reservoir intervals in the Curimã and Espada fields are thinner than 20 m. Thus, one seismic reflection in the interpreted seismic volume may represent several porous layers with reservoir potential. Accordingly, we can suggest the future development of a 3D geological model of the area using sequence stratigraphic concepts (e.g. Catuneanu, 2006; Martins-Neto and Catuneanu, 2010; Holz et al., 2017). A 3D reservoir model using geostatistic numerical models should be used in a second stage as a basis for simulation and fluid flow analysis (Consentino, 2001). These two latter approaches will be crucial to plan the development of the oil fields referred to in this work.

6. Conclusions

Three-dimensional (3D) structural modelling integrating a seismic cube and well data from the Mundaú sub-basin, including part of the Espada field and the entire Curimã field, was developed in this research. This work introduced a variety of plays from an oil producing region of the Brazilian Equatorial Margin expanding the possibility of future discoveries in this area and also in the Guyana-Suriname-French Guiana system and Equatorial Africa as a whole. The findings in this research have focused on subtle stratigraphic traps. In addition, we also assess the importance of structural and combined plays, challenging academia and industry to consider these play types as crucial in Equatorial margins of the Central Atlantic; we emphasize here that the 79% of giant fields in the world are structural plays (Dolson et al., 2018). Main conclusions are as follows:

a) Extensional faults in the study area are planar at depth, seaward-dipping, and revealing a NW-SE strike direction and a NE dip direction. They present an *en echelon* geometry and are responsible for stepping and tilting of crustal blocks (half-grabens) during the syn-rift phase. Faults were active until the beginning of the drift phase. Some of them root into the basement while others reach the top of Unit 1.
b) Seismic interpretation indicates transcurrent movement in the mapped faults, recorded in the form of abrupt change in seismic facies across faults, changes from normal to reverse along their strike and with depth, changes in thickness and intensity of seismic reflections across faults, and synclines and anticlines formed between faults. Strike-slip tectonics reflects the nearby presence of transtensional fault systems associated with oblique rifting in the Equatorial Atlantic.
c) In the study area are found important oil accumulations in combined, structural and stratigraphic plays.

Combined plays are formed by Aptian reservoirs in blocks tilted by Faults 6 and 7, and the deposition of the transgressive shales of Unit 6 (Uruburetama Mb.) above an erosional unconformity. It is worth stressing the importance of not completely eroding the transitional Unit 5 (Paracuru Formation), which contains better reservoirs in the study area, as well as the Uruburetama Member, sealing underlying reservoir intervals. The basement structure controlled deposition during the syn-rift and transitional stages. In addition, the structural high in the SE part of the area was largely removed by an erosional event after the transitional phase, contributing to erosion of the Unit 5 and, consequently, the failure of some exploratory wells. This type of play is also found in the African conjugate margin represented by Espoir and Baobab fields in Ivory Coast Basin.

Structural plays comprise anticlinal traps on the hanging-wall block tilted by Fault 7 (Curimã Fault). The Côte D'Ivoire-Ghana transform margin presents this type of play, which is related to transform structures at the end of large Fracture Zones.

Stratigraphic plays consist of Upper Cretaceous turbidite sandstones intercalated with shales. Here, faults are not important traps. However, they are responsible for oil migration. Very important

discoveries in Stabroek block in Guyana and in Gulf of Guinea were assigned to this type of play.

In summary, the mapping of faults and traps in this work reveals the importance of a multi-faceted structural component to the entrapment of hydrocarbons in the Mundaú sub-basin. These results can assist further geological modelling in the Brazilian Equatorial Margin and, consequently, reservoir simulations in order to plan the development of proven and future oil fields. The structural model presented here is a starting point to further exploration work in the remainder of the Brazilian Equatorial Margin and on the conjugate Equatorial African margin.

Author contribution

Maia de Almeida, Narelle: Term, Conceptualization, Formal analysis, Investigation, Visualization, Writing - original draft, Writing - review & editing, Visualization, Supervision; Alves, Tiago M.: Term, Conceptualization, Formal analysis, Investigation, Visualization, Writing - original draft, Writing - review & editing, Visualization; Nepomuceno Filho, F: Project administration, Resources, Supervision, Writing - review & editing; Freire, George Satander Sá: Supervision, Writing - review & editing; Souza, Ana Clara B.: Formal analysis, Writing - review & editing; Leopoldino Oliveira, Karen M: Writing - review & editing; Normando, Márcio Nunes: Writing - review & editing; Barbosa, Thiago Henrique S: Data curation, Writing - review & editing.

Declaration of competing interest

The authors declare that they have no known competing financial interests or personal relationships that could have appeared to influence the work reported in this paper.

Acknowledgements

The authors are grateful to the Brazilian National Petroleum Agency for providing seismic and well data, and to Schlumberger for their software licenses. The authors also thank Cardiff University (3D Seismic Lab) and the Coordenação de Aperfeiçoamento de Pessoal de Nível Superior (CAPES) for an exchange period of the first author in 2017, and the Federal University of Ceará (Laboratórios de Interpretação Sísmica e de Geologia Marinha e Aplicada) for their support to this study. This study was financed in part by CAPES, Brazil, Finance Code 001. The authors are grateful to the reviewers for their comments to earlier versions of this work.

References

Alves, T.M., Cunha, T.A., 2018. A phase of transient subsidence, sediment bypass and deposition of regressive–transgressive cycles during the breakup of Iberia and Newfoundland. Earth Planet Sci. Lett. 484, 168–183.

Andrade, J.F.P., Gomes, M.P., Bezerra, F.R., Castro, D.L., Vital, H., 2018. Morphotectonic development of the Ceará terrace: a marginal ridge on the western side of the Romanche fracture zone in the Brazilian equatorial margin. Geo Mar. Lett. https://doi.org/10.1007/s00367-018-0541-y. (Accessed 12 July 2018).

ANP, 2013. Sumário Executivo do Campo de Espada. Contrato de Concessão n° 48000.003777/97-31. Plano de Desenvolvimento aprovado na Reunião de Diretoria n° 718 de 18/07/2013, Resolução de Diretoria n° 715/2013, 2 pp.

ANP, 2016. Sumário Executivo do Campo de Curimã. Plano de Desenvolvimento Aprovado. Reunião de Diretoria nº 812 de 07/08/2015, Resolução nº 584/2015. Agência Nacional do Petróleo, Gás Natural e Biocombustíveis (ANP), 3 pp.

ANP, 2017a. BACIA DO CEARÁ, Sumário Geológico e Setores em Oferta. Ildeson Prates Bastos. Superintendência de Definição de Blocos – SDB. Rodada 15. Brasil, Concessões de Petróleo e Gás. Agência Nacional do Petróleo. Gás Natural e Biocombustíveis (ANP), p. 17.

ANP, 2017b. BACIA POTIGUAR, Sumário Geológico e Setores em Oferta. Carlos Mikael Arnemann Batista. Superintendência de Definição de Blocos – SDB. Rodada 15. Brasil, Concessões de Petróleo e Gás. Agência Nacional do Petróleo. Gás Natural e Biocombustíveis (ANP), p. 17.

ANP, 2018. BACIA POTIGUAR. 15ª Rodada de Licitação da Agência Nacional do Petróleo, Gás Natural e Biocombustíveis. Superintendência de Definição de Blocos. Por Carlos Mikael Arnemann Batista.

ANP, 2020. Painel Dinâmico da Agência Nacional do Petróleo, Gás Natural e Biocombustíveis. http://www.anp.gov.br/exploracao-e-producao-de-oleo-e-gas/painel-dinamico-de-producao-de-petroleo-e-gas-natural.

Antunes, A.F., 2004. Evolução tectono-estrutural do campo de Xaréu (Sub-bacia Mundaú, Bacia do Ceará – NE do Brasil): abordagem multiescala e pluriferramental. Tese de Doutorado. Programa de Pós-Graduação em Geodinâmica e Geofísica, Universidade Federal do Rio Grande do Norte, Natal, p. 376.

Antunes, A.F., Jardim de Sá, E.F., Araújo, R.G.S., Lima Neto, F.F., 2008. Caracterização tectonoestrutural do Campo de Xaréu (Sub-Bacia de Mundaú, Bacia do Ceará – NE do Brasil): abordagem multiescala e pluriferramental. Rev. Bras. Geociencias 38 (1 - Suppl. o), 88–105.

Attoh, K., Brown, L., Guo, J., Heanlein, J., 2004. Seismic stratigraphic record of transpression and uplift on the Romanche transform margin, offshore Ghana. Tectonophysics 378 (2004), 1–16. https://doi.org/10.1016/j.tecto.2003.09.026.

Azevedo, R.P., 1991. Tectonic Evolution of Brazilian Equatorial Continental Margin Basins. Phd. Thesis. Imperial College London (University of London), London, UK, p. 535.

Basile, C., Mascle, J., Guiraud, R., 2005. Phanerozoic geological evolution of the Equatorial Atlantic domain. J. Afr. Earth Sci. 43, 275–282. https://doi.org/10.1016/j.jafrearsci.2005.07.011.

Beltrami, C.V., Alves, L.E.M., Feijó, F.J., 1994. Bacia do Ceará. In: Boletim de Geociências da Petrobras, vol. 8, p. 117–125 n.1.

Brandes, C., Tanner, D.C., 2014. Fault-related folding: a review of kinematic models and their application. Earth Sci. Rev. 138, 352–370.

Bridwell, R.J., 1975. Sinuosity of strike-slip fault traces. Geology 3 (11), 630–632. https://doi.org/10.1130/0091-7613(1975)3<630:SOSFT>2.0.CO;2.

Brooks, J., Glennie, K.W., 1987. Petroleum Geology of North West Europe. Graham & Trotman, London.

Brownfield, M.E., Charpentier, R.R., 2006. Geology and total petroleum systems of the Gulf of Guinea Province of west Africa. U.S Geological Survey Bulletin 2207-C 32.

Castro, A. S. de, 1993. Arcabouço Estrutural e Evolucão Tectônica da Sub-Bacia de Icaraí, Bacia do Ceará. Unpublished Master's thesis. Universidade Federal Ouro Preto, Brazil.

Catuneanu, O., 2006. Principles of Sequence Stratigraphy. Elsevier, p. 375.

Condé, V.C., Lana, C.C., Pessoa Neto, O.C., Roesner, E.H., Morais Neto, J.M., Dutra, D.C., 2007. Bacia do Ceará. In: Boletim de Geociências da Petrobras, Rio de Janeiro, vol. 15, pp. 347–355, 2 (maio/nov).

Consentino, L., 2001. Integrated Reservoir Studies. Institut Français du Pétrole Publications. Editons Technip, Paris, p. 336.

Corfield, S., Sharp, I., 2000. Structural style and stratigraphic architecture of fault propagation folding in extensional settings: a seismic example from the Smørbukk area. Halten Terrace, Mid-Norway: Basin Res. 12 (3-4), 329–341.

Costa, I.G., Beltrami, C.V., Alves, L.E.M., 1990. A evolução tectono-sedimentar e o "habitat" do óleo na Bacia do Ceará. Bol. Geociencias Petrobras 4 (1), 65–74.

Dailly, P., Henderson, T., Hudgens, E., Kanschat, K., Lowry, P., 2013. Exploration for cretaceous stratigraphic traps in the Gulf of Guinea, west Africa and the discovery of the jubilee field: a play opening discovery in the Tano Basin, offshore Ghana. In: Mohriak, W.U., Danforth, A., Post, P.J., Brown, D.E., Tari, G.C., Nemčok, M., Sinha, S.T. (Eds.), Conjugate Divergent Margins, vol. 369. Geological Society, London, Special Publications, pp. 235–248. https://doi.org/10.1144/SP369.12.

Dailly, P., Henderson, T., Kanschat, K., Lowry, P., Sills, S., 2017. The jubilee field, Ghana: opening the late cretaceous play in the west african transform margin. Memoir. In: Giant Fields of the Decade 2000-2010, 2017 (Chapter 14). AAPG Special Volumes, vol. 113, pp. 257–272. https://doi.org/10.1306/13572010M1132997.

Davison, I., Faull, T., Greenhalgh, J., Beirne, E.O., Steel, I., 2016. Transpressional structures and hydrocarbon potential along the Romanche Fracture Zone: a review. In: Nemčok, M., Rybar, S., Sinha, S.T., Hermeston, S.A., Ledvenyiova, L. (Eds.), Transform Margins: Development, Controls and Petroleum Systems: London, vol. 431. Geological Society, Special Publications, pp. 235–248.

Deng, Q., Wu, D., Zhang, P., Chen, S., 1986. Structure and deformational character of strike-slip fault zones. Pure Appl. Geophys. 124 (1–2), 203–223.

Dolson, J., He, Z., Horn, B.W., 2018. Advances and perspectives on stratigraphic trap exploration-making the subtle trap obvious. Search and discovery article #60054 (2018). In: AAPG 2017 Middle East Region Geosciences Technology Workshop, Stratigraphic Traps of the Middle East, Muscat, Oman, December 11-13, 2017, p. 67.

Exxon Mobil, 2020. Guyana project overview. Article Feb. 5, 2020. https://corporate.exxonmobil.com/Locations/Guyana/Guyana-project-overview#DiscoveriesintheStabroekBlock. (Accessed 9 May 2020).

Fossen, H., 2016. Structural Geology, second ed. Cambridge University Press, ISBN 978-1-107-05764-7, p. 452.

Fossen, H., Teyssier, C., Whitney, D.L., 2013. Transtensional folding. J. Struct. Geol. 56, 89–102.

Françolin, J.B.L., Szatmari, P., 1987. Mecanismo de rifteamento da porção oriental da margem norte brasileira. Rev. Bras. Geociencias 17, 196–207.

Gorini, M.A., 1993. A margem equatorial brasileira: uma visão geotectônica: resumos expandidos do Congresso Internacional da Sociedade Brasileira de Geofísica 3. Sociedade Brasileira de Geofísica 2, 1355–1357.

Goss, S., Mosher, D., Wach, G.D., 2008. Continental margin development of the equatorial Atlantic gateway: Suriname, South America. In: Central Atlantic Conjugate Margins Conference, Halifax, pp. 282–291.

Hardman, R.F.P., Booth, J.E., 1991. The significance of normal faults in the exploration and production of North Sea hydrocarbons. In: Roberts, A.M., Yielding, G., Freeman, B. (Eds.), The Geometry of Normal Faults, vol. 56. Geological Society Special Publication No, pp. 1–13.

Heine, C., Brune, S., 2014. Oblique rifting of the equatorial atlantic: why there is no saharan Atlantic Ocean. Geology 42 (3), 211–214. https://doi.org/10.1130/G35082.1, 2014.
Hempton, M.R., Neher, K., 1986. Experimental fracture, strain and subsidence patterns over en échelon strike-slip faults: implications for the structural evolution of pull-apart basins. J. Struct. Geol. https://doi.org/10.1016/0191-8141(86)90066-0.
Hoerlle, M.R., Gomes, C.J.S., Matos, R.M.D., 2007. O Graben de Apodi, região sudoeste da bacia Potiguar, RN, uma interpretação com base em seções sísmicas e dados de poços. R. Esc. Minas, Ouro Preto 60 (4), 593–602.
Holz, M., Vilas-Boas, D.B., Troccoli, E.B., Santana, V.C., Vidigal-Souza, P.A., 2017. Conceptual models for sequence stratigraphy of continental rift successions. Stratigraphy & Timescales 2, 119–186.
Howard, K.A., John, B.E., 1997. Fault-related folding during extension: plunging basement-cored folds in the Basin and Range. Geology 25 (3), 223–226.
Huaicun, J., 2014. Progress and revelation of exploration of large oil and gas fields around the globe. Sci. Technol. Rev. 32 (8), 76–83, 2014.
Illing, L.V., Hobson, G.C., 1981. Petroleum Geology of the Continental Shelf of North-West Europe. institute of Petroleum, Heyden, London.
Jiang, H., Pang, X., Shi, H., Liu, L., Bai, J., Zou, S., 2015. Effects of Fault activities on hydrocarbon migration and accumulation in the zhu I depression, pearl river mouth basin, south China Sea. Aust. J. Earth Sci. 62 (6), 775–788. https://doi.org/10.1080/08120099.2015.1101400.
Jianping, L., Xiaohua, P., Jun, M., Zuoji, T., Lunkun, W., 2010. Exploration targets in the Côte d'Ivoire-Ghana transform margin in equatorial west Africa. PETROL. EXPLOR. DEVELOP. 37 (1), 43–50, 2010.
Jin, G., Groshong, R.H., 2006. Trishear kinematic modeling of extensional fault propagation folding. J. Struct. Geol. 28 (1), 170–183.
Kelly, J., Doust, H., 2016. Exploration for late cretaceous turbidites in the equatorial african and northeast south American margins. Netherlands Journal of Geosciences - Geologie en Mijnbouw 95 (4), 393–403. https://doi.org/10.1017/njg.2016.36.
Khalil, S., McClay, K., 2002. Extensional fault-related folding, northwestern Red Sea, Egypt. J. Struct. Geol. 24 (4), 743–762.
Knipe, R.J., Jones, G., Fisher, Q.J., 1998. Faulting, fault sealing and fluid flow in hydrocarbon reservoirs: an introduction. In: Jones, G., Fisher, Q.J., Knipe, R.J. (Eds.), Faulting, Fault Sealing and Fluid Flow in Hydrocarbon Reservoirs, vol. 147. Geological Society, London, Special Publications pp. vii–xxi.
Lamarche, G., Basile, C., Mascle, J., Sage, F., 1997. The Côte d'Ivoire–Ghana transform margin: sedimentary and tectonic structure from multichannel seismic data. Geo Mar. Lett. 17, 62–69.
Leopoldino Oliveira, K.M., Bedle, H., Branco, R.M.G.C., de Souza, A.C.B., Nepomuceno Filho, F., Nomando, M.N., Maia de de Almeida, N., da Silva Barbosa, T.H., 2020. Seismic stratigraphic patterns and characterization of deepwater reservoirs of the Mundaú sub-basin, Brazilian Equatorial Margin. Mar. Petrol. Geol. https://doi.org/10.1016/j.marpetgeo.2020.104310.
Loncke, L., Maillard, A., Basile, C., Roest, W.R., Bayon, G., Gaullier, V., Pattier, F., Mercier De Le Pinay, M., Grall, C., Droz, L., Marsset, T., Giresse, P., Caprais, J.C., Cathalot, C., Graindorge, D., Heuret, A., Lebrun, J.F., Bermell, S., Marcaillou, B., Sotin, C., Hebert, B., Patriat, M., Bassetti, M.A., Tallobre, C., Buscail, R., Durrieu De Madron, X., Bourrin, F., 2016. Structure of the Demerara passive-transform margin and associated sedimentary processes. Initial results from the IGUANES cruise. From. In: Nemcok, M., Rybar, S., Sinha, S.T., Hermeston, S.A., Ledvenyiova, L. (Eds.), 2016.Transform Margins: Development, Controls and Petroleum Systems, vol. 431. Geological Society, London,Special Publications, pp. 179–197. https://doi.org/10.1144/SP431.7. First published online December 14, 2015.
Lonsdale, P., 1989. Segmentation of the Pacific-Nazca spreading center, 1-DEGREESN-20-DEGREES-S. J. Geophy. Res.-solid Earth 94 (B9), 12197–12225. https://doi.org/10.1029/JB094iB09p12197.
Maia de Almeida, N.M., Alves, T.M., Nepomuceno Filho, F., Freire, G.S.S., Souza, A.C.B., Normando, M.N., Oliveira, K.M.L., Barbosa, T.H.S., 2020. Tectono-sedimentary evolution and petroleum systems of the Mundaú sub-basin: a new deep-water exploration frontier in equatorial Brazil. AAPG (Am. Assoc. Pet. Geol.) Bull. 104 (4), 795–824. https://doi.org/10.1306/07151917381. April 2020.
Martins-Neto, M.A., Catuneanu, O., 2010. Rift sequence stratigraphy. Mar. Petrol. Geol. 27 (1), 247–253.
Matos, R.M.D., Waick, R.N., Pimentel, V.P.C., 1996. Bacia do Ceará (Mundaú): uma fase rifte convencional!?. In: SBG/Núcleo Bahia-Sergipe, Congr. Bras. Geol., vol. 39. Anais, pp. 358–362, 5.
Matos, R.M.D., 2000. Tectonic evolution of the equatorial south Atlantic. In: Mohriak, W., Talwani, M. (Eds.), Atlantic Rifts and Continental Margins. American Geophysical Union, Washington, D.C., pp. 331–354
Mcclay, K.R., Scott, A.D., 1991. Experimental models of hangingwall deformation in ramp-flat listric extensional fault systems. Tectonophysics 188, 85–96.
Medeiros, W.E., Nascimento, A.F., Antunes, A.F., Emanuel Ferraz Jardim de Sá, E.F.J., Lima Neto, F.F., 2007. Spatial Pressure Compartmentalization in Faulted Reservoirs as a Consequence of Fault Connectivity: a Fluid Flow Modelling Perspective. Xaréu oil field, NE Brazil.
Milani, E.J., Brandão, J.A.S.L., Zalán, P.V., Gamboa, L.A.P., 2000. Petróleo na margem continental brasileira: geologia, exploração, resultados e perspectivas. Braz. J. Genet. 18, 352–396. https://doi.org/10.1590/S0102-261X2000000300012.
Mitchum, R.M., Vail, P.R., Thompson, S., 1977. Seismic stratigraphy and global changes of Sea level, Part 2: the depositional sequence as a basic unit for stratigraphic analysis. In: Seismic Stratigraphy Applied to Hydrocarbon Exploration, vol. 26. AAPG Memoir, pp. 53–62.
Mohriak, W.U., 2003. Bacias sedimentares da margem continental brasileira. In: Bizzi, L. A., Schobbenhaus, C., Vidotti, R.M., Golçalves, J.H. (Eds.), Geologia, tectônica e recursos minerais do Brasil: textos, mapas & SIG. CPRM, Brasília, pp. 87–165.
Morais Neto, J.M., Pessoa Neto, O.C., Lana, C.C., Zalán, P.V., 2003. Bacias sedimentares brasileiras: bacia do Ceará. Phoenix. Aracaju 57, 1–6.
Moustafa, A.R., Abd-Allah, A.M., 1992. Transfer zones with en echelon faulting at the northern end of the Suez Rift. Tectonics, AGU Journal 11 (3), 499–506. https://doi.org/10.1029/91TC03184.
Nemčok, M., Rybar, S., Odegard, M., Dickson, W., Pelech, O., LedveNyiova, L., Matejova, M., Molc, M., Hermeston, S., Jones, D., Cuervo, E., Cheng, R., Forero, G., 2016a. Development history of the southern terminus of the Central Atlantic: Guyana–Suriname case study. From. In: Nemčok, M., Rybár, S., Sinha, S.T., Hermeston, S.A., Ledvenyiova, L. (Eds.), 2016. Transform Margins: Development, Controls and Petroleum Systems, vol. 431. Geological Society, London, Special Publications, pp. 145–178. https://doi.org/10.1144/SP431.10. First published online December 14, 2015.
Nemčok, M., Rybár, S., Ekkertová, P., Kotulová, J., Hermeston, S.A., Jones, D., 2016b. Transform-margin model of hydrocarbon migration: the Guyana–Suriname case study. From. In: Nemčok, M., Rybár, S., Sinha, S.T., Hermeston, S.A., Ledvényiová, L. (Eds.), 2016. Transform Margins: Development, Controls and Petroleum Systems, vol. 431. Geological Society, London, Special Publications, pp. 199–217. https://doi.org/10.1144/SP431.6. First published online December 14, 2015.
Nemčok, M., Rybár, S., Sinha, S.T., Hermeston, S.A., Ledvényiova, L., 2016c. Transform margins: development, controls and petroleum systems – an introduction. From. In: Nemčok, M., Rybár, S., Sinha, S.T., Hermeston, S.A., Ledvényiová, L. (Eds.), Transform Margins: Development, Controls and Petroleum Systems, vol. 431. Geological Society, London, Special Publications. https://doi.org/10.1144/SP431.15.
Nemčok, M., 2016. Rifts and Passive Margins: Structural Architecture, Thermal Regimes and Petroleum Systems. Cambridge University Press, p. 607.
Offshore, 2020. https://www.offshore-technology.com/projects/liza-prospect-development-stabroek-block/.
OGJ, 2020. In: Oil and Gas Journal. ExxonMobil Confirms Oil Discovery in Second Well Offshore Guyana. https://www.ogj.com/articles/2016/06/exxonmobil-confirms-oil-discovery-in-second-well-offshore-guyana.html.
Pellegrini, B.S., Severiano Ribeiro, H.J.P., 2018. Exploratory plays of Pará-Maranhão and Barreirinhas basins in deep and ultra-deep waters, Brazilian Equatorial Margin. Braz. J. Genet. 48 (3), 485–502. https://doi.org/10.1590/2317-4889201820180146.
Pessoa Neto, O.C., 2004. Blocos basculados truncados por discordância angular: lições aprendidas em trapeamento combinado de hidrocarbonetos, Bacia do Ceará, Nordeste do Brasil, vol. 12. Boletim de Geociências Petrobras, Rio de Janeiro, pp. 59–71, 1.
Sauerbronn, J.L.B., 1996. Transição Crustal e Evolução Tectônica do Segmento Transformante da Margem Equatorial Brasileira, adjacente à Bacias de Barreirinhas e do Ceará. Master's thesis. Universidade Federal Ouro Preto, Brazil.
Scarselli, N., Duval, G., Martin, J., Mcclay, K., Toothill, S., 2018. Insights into the early evolution of the Côte d'Ivoire margin (west Africa). From. In: Mcclay, K.R., Hammerstein, J.A. (Eds.), Passive Margins: Tectonics, Sedimentation and Magmatism, vol. 476. Geological Society, London, Special Publications. https://doi.org/10.1144/SP476.8.
Sharp, I.R., Gawthorpe, R.L., Underhill, J.R., Gupta, S., 2000. Fault-propagation folding in extensional settings: examples of structural style and synrift sedimentary response from the Suez rift, Sinai, Egypt. Geol. Soc. Am. Bull. 112 (12), 1877–1899.
Soares, D., Alves, T.M., Terrinha, P., 2012. The breakup sequence and associated lithospheric breakup surface: their significance in the context of rifted continental margins (West Iberia and Newfoundland margins, North Atlantic). Earth Planet Sci. Lett. 355–356, 311–326.
Soares Júnior, A.V., Hasui, Y., Costa, J.B.S., Machado, F.B., 2011. Evolução do Rifteamento e Paleogeografia da Margem Atlântica Equatorial do Brasil: triássico ao Holoceno. São Paulo, UNESP, Geociências 30 (4), 669–692.
Szatmari, P., Françolin, J.B., Zanotto, O., Wolff, S., 1987. Evolução tectônica da margem equatorial brasileira. Rev. Bras. Geociencias 17, 180–188.
Tetteh, J.T., 2016. The cretaceous play of Tano Basin, Ghana. Int. J. Appl. Sci. Technol. 6 (No. 1). February 2016. ISSN 2221-0997 (Print), 2221-1004 (Online).
Ward, N.I.P., Alves, T.M., Blenkinsop, T.G., 2016. Submarine sediment routing over a blocky mass-transport deposit in the Espírito Santo Basin, SE Brazil. Basin Res. 30 (4), 816–834.
Ward, N.I.P., Alves, T.M., Blenkinsop, T.G., 2018. Differential compaction over Late Miocene submarine channels in SE Brazil: implications for trap formation. GSA Bulletin 130 (1–2), 208–221.
Withjack, M.O., Olson, J., Peterson, E., 1990. Experimental models of extensional forced folds. AAPG (Am. Assoc. Pet. Geol.) Bull. 74 (7), 1038–1054.
Watts, A.B., Rodger, M., Peirce, C., Greenroyd, C.J., Hobbs, R.W., 2009. Seismic structure, gravity anomalies, and flexure of the Amazon continental margin, NE Brazil. J. Geophys. Res. 114, B07103. https://doi.org/10.1029/2008JB006259.
Yang, W., Escalona, A., 2011. Tectonostratigraphic evolution of the Guyana basin. AAPG (Am. Assoc. Pet. Geol.) Bull. 95 (8), 1339–1368. https://doi.org/10.1306/01031110106. August 2011.
Yielding, G., 1990. Footwall uplift associated with late jurassic normal faulting in the northern north Sea. Journal of the Geological Society of London 147, 219–222.
Zachariasen, J., Sieh, K., 1995. The transfer of slip between two en echelon strike-slip faults: a case study from the 1992 Landers earthquake, southern California. J. Geophys. Res. 100 (B8), 15,281–15,301.
Zálan, P.V., Warme, J.E., 1985. Tectonics and Sedimentation of the Piauí-Camocim Sub-basins, Ceará Basin, Offshore Northeastern Brazil: Série Ciência-Técnica-Petróleo (17). Petrobras, Rio de Janeiro, p. 71.
Zalán, P.V., 1986. Identificação de falhas transcorrentes em seções sísmicas. Rev. Bras. Geociencias 16 (3), 258–265.

Zalán, P.V., 2004. Evolução fanerozóica das bacias sedimentares brasileiras. In: Mantesso-Neto, V., Bartorelli, A., Carneiro, C.D.R., Brito Neves, B.B.B. (Eds.), Geologia do continente sul-americano: evolução da obra de Fernando Flávio Marques de Almeida. Editora Beca, São Paulo, pp. 595–612.

Zalán, P.V., 2015. Similarities and differences between magma-poor and volcanic passive margins – applications to the Brazilian marginal basins. In: Conference Paper - 14th International Congress of the Brazilian Geophysical Society held in Rio de Janeiro, Brazil, pp. 37–42. https://doi.org/10.1190/sbgf2015-007.

Zalán, P.V., Neil, H., Saunders, M., 2019. Foz do Amazonas and pará-maranhão basins ready to replicate Guyana success. Search and discovery article #30624. In: AAPG Annual Convention and Exhibition, San Antonio, Texas, May 19-22, 2019. https://doi.org/10.1306/30624Zalan2019.

Zhang, G., Qu, H., Chen, G., Zhao, C., Zhang, F., Yang, H., Zhao, Z., Ma, M., 2019. Giant discoveries of oil and gas fields in global deepwaters in the past 40 years and the prospect of exploration. Journal of Natural Gas Geoscience 4 (2019), 1–28. https://doi.org/10.1016/j.jnggs.2019.03.002.